

Merging cranial histology and 3D-computational biomechanics: a review of the feeding ecology of a Late Triassic temnospondyl amphibian (#19988)

1

First submission

Please read the **Important notes** below, the **Review guidance** on page 2 and our **Standout reviewing tips** on page 3. When ready [submit online](#). The manuscript starts on page 4.

Important notes

Editor and deadline

Claudia Marsicano / 21 Sep 2017

Files

8 Figure file(s)

2 Table file(s)

1 Other file(s)

Please visit the overview page to [download and review](#) the files not included in this review PDF.

Declarations

No notable declarations are present



Please read in full before you begin

How to review

When ready [submit your review online](#). The review form is divided into 5 sections. Please consider these when composing your review:

- 1. BASIC REPORTING**
- 2. EXPERIMENTAL DESIGN**
- 3. VALIDITY OF THE FINDINGS**
4. General comments
5. Confidential notes to the editor

 You can also annotate this PDF and upload it as part of your review

To finish, enter your editorial recommendation (accept, revise or reject) and submit.

BASIC REPORTING

-  Clear, unambiguous, professional English language used throughout.
-  Intro & background to show context. Literature well referenced & relevant.
-  Structure conforms to [PeerJ standards](#), discipline norm, or improved for clarity.
-  Figures are relevant, high quality, well labelled & described.
-  Raw data supplied (see [PeerJ policy](#)).

EXPERIMENTAL DESIGN

-  Original primary research within [Scope of the journal](#).
-  Research question well defined, relevant & meaningful. It is stated how the research fills an identified knowledge gap.
-  Rigorous investigation performed to a high technical & ethical standard.
-  Methods described with sufficient detail & information to replicate.

VALIDITY OF THE FINDINGS

-  Impact and novelty not assessed. Negative/inconclusive results accepted. *Meaningful* replication encouraged where rationale & benefit to literature is clearly stated.
-  Conclusions are well stated, linked to original research question & limited to supporting results.
-  Speculation is welcome, but should be identified as such.
-  Data is robust, statistically sound, & controlled.

The above is the editorial criteria summary. To view in full visit <https://peerj.com/about/editorial-criteria/>

7 Standout reviewing tips

3



The best reviewers use these techniques

Tip

Example

Support criticisms with evidence from the text or from other sources

Smith et al (J of Methodology, 2005, V3, pp 123) have shown that the analysis you use in Lines 241-250 is not the most appropriate for this situation. Please explain why you used this method.

Give specific suggestions on how to improve the manuscript

Your introduction needs more detail. I suggest that you improve the description at lines 57- 86 to provide more justification for your study (specifically, you should expand upon the knowledge gap being filled).

Comment on language and grammar issues

The English language should be improved to ensure that your international audience can clearly understand your text. I suggest that you have a native English speaking colleague review your manuscript. Some examples where the language could be improved include lines 23, 77, 121, 128 - the current phrasing makes comprehension difficult.

Organize by importance of the issues, and number your points

1. Your most important issue
2. The next most important item
3. ...
4. The least important points

Give specific suggestions on how to improve the manuscript

Line 56: Note that experimental data on sprawling animals needs to be updated. Line 66: Please consider exchanging "modern" with "cursorial".

Please provide constructive criticism, and avoid personal opinions

I thank you for providing the raw data, however your supplemental files need more descriptive metadata identifiers to be useful to future readers. Although your results are compelling, the data analysis should be improved in the following ways: AA, BB, CC

Comment on strengths (as well as weaknesses) of the manuscript

I commend the authors for their extensive data set, compiled over many years of detailed fieldwork. In addition, the manuscript is clearly written in professional, unambiguous language. If there is a weakness, it is in the statistical analysis (as I have noted above) which should be improved upon before Acceptance.

Merging cranial histology and 3D-computational biomechanics: a review of the feeding ecology of a Late Triassic temnospondyl amphibian

Dorota Konietzko-Meier ^{Corresp., 1, 2}, Kamil Gruntmejer ^{2, 3}, Jordi Marcé-Nogué ⁴, Adam Bodzioch ², Josep Fortuny ^{5, 6}

¹ Steinmann Institute, University of Bonn, Bonn, Germany

² Department of Biosystematics, University of Opole, Opole, Poland

³ European centre of Palaeontology, University of Opole, Opole, Poland

⁴ Centre of Natural History, University of Hamburg, Hamburg, Germany

⁵ Virtual Paleontology Department, Institut Català de Paleontologia M. Crusafont., Cerdanyola del Vallès, Spain

⁶ Centre de Recherches en Paléobiodiversité et Paléoenvironnements, Muséum national d'Histoire naturelle, Paris, France

Corresponding Author: Dorota Konietzko-Meier

Email address: dorotam@uni.opole.pl

A useful method for understanding form and function is Finite Element Analysis. However, modelling of fossil taxa invariably involves assumptions as a result of preservation-induced loss of information in the fossil record. To test the validity of such assumptions a sensitive method is needed, e.g., bone and suture microstructure. The bony framework is a product of biological optimisation; bone structure is created to meet local mechanical conditions. Thus, bone microstructure can be used to recalculate local stress and these results can be combined with the Finite Element models. To test this scenario, the early tetrapod group of Temnospondyli is an excellent case-study. This clade ranks amongst the most important groups of extinct amphibians during the Early Carboniferous to late Early Cretaceous. In spite of the fact that they have been intensively studied during the last century a half their biology and mode of life still are debated. A crucial issue is their feeding mode; did they suction feed or employ direct biting, or both. The genus *Metoposaurus*, which is very common in Upper Triassic strata, is a good model for testing the various hypotheses about feeding strategies. Metoposaurids have previously been characterised either as active hunters or passive bottom dwellers. In order to assess assumptions required for Finite Element Analyses, two skulls of *Metoposaurus krasiejowensis* from the Upper Triassic of southwest Poland were tested accordingly and microscopical observations of dermal bone microstructure and suture morphology in 39 thin sections were added. For the first time, three independent models were merged in a revision of the feeding strategy of *Metoposaurus*. *Metoposaurus* appears to have been an aquatic animal that was little specialised concerning feeding behaviour. This taxon may have used two foraging

techniques in hunting; an ambush strategy, using bilateral biting, or active hunting, using lateral strikes of the head. However, microscopic data suggest that lateral biting was commoner than can be observed in Finite Element Analysis only. The main factor that determined its mode of life probably was water levels. During optimum water conditions, metoposaurids were active ambush predators capable of lateral strikes of the head. The dry season required a less active mode of life with particularly efficient bilateral biting and, combined with their characteristically anteriorly positioned orbits, optimal for ambush strategy. This ability for food acquisition, independent of environmental conditions, could be the key to explain the very common occurrence of metoposaurids during the Late Triassic

1 Merging cranial histology and 3D-computational biomechanics: a review of the feeding ecology
2 of a Late Triassic temnospondyl amphibian

3

4 Dorota Konietzko-Meier^{1,2,*}, Kamil Gruntmejer^{2,3}, Jordi Marcé-Nogué⁴, Adam Bodzioch², Josep
5 Fortuny^{5,6}

6

7 ¹Steinmann Institute, University of Bonn, Nussallee 8, 53115 Bonn, Germany

8 ²Department of Biosystematics, Opole University, Oleska 22, 45-052 Opole, Poland

9 ³European Centre of Palaeontology, Oleska 48, 45-052 Opole, Poland

10 ⁴Centre of Natural History (CeNak), University of Hamburg, Martin-Luther-King-Platz 3,
11 20146 Hamburg, Germany

12 ⁵Institut Català de Paleontologia Miquel Crusafont, ICTA-ICP Building, c/ de les Columnes, s/n,
13 08193 Cerdanyola del Vallès, Spain

14 ⁶Centre de Recherches en Paléobiodiversité et Paléoenvironnements, Muséum national
15 d'Histoire naturelle, Bâtiment de Paléontologie, CP38, 8 rue Buffon, 75005 Paris, France

16 * Address for correspondence (E-mail: dorotam@uni.opole.pl)

17

18

19

20

21

22

23

24

25 ABSTRACT

26 A useful method for understanding form and function is ~~Finite Element Analysis~~. However,
27 modelling of fossil taxa invariably involves assumptions as a result of preservation-induced loss
28 of information in the fossil record. To test the validity of such assumptions a sensitive method is
29 needed, e.g., bone and suture microstructure. The bony framework is a product of biological
30 optimisation; bone structure is created to meet local mechanical conditions. Thus, bone
31 microstructure can be used to ~~recalculate~~ local stress and these results can be combined with the
32 Finite Element models. To test this scenario, the early tetrapod group of Temnospondyli is an
33 excellent case-study. This clade ranks among ~~st~~ the most important groups of extinct amphibians
34 during the Early Carboniferous to late Early Cretaceous. In spite of the fact that they have been
35 intensively studied during the last ~~century a half~~, their biology and mode of life still are debated.
36 A crucial issue is their feeding mode; did they suction feed or employ direct biting, or both. The
37 genus *Metoposaurus*, which is very common in Upper Triassic strata, is a good model for testing
38 the various hypotheses about feeding strategies. Metoposaurids have previously been
39 characterised either as active hunters or passive bottom dwellers. In order to assess assumptions
40 required for Finite Element Analyses, two skulls of *Metoposaurus krasiejowensis* from the
41 Upper Triassic of southwest Poland were tested accordingly and microscopical observations of
42 dermal bone microstructure and suture morphology in 39 thin sections were added. For the first
43 time, three independent models were merged in a revision of the feeding strategy of
44 *Metoposaurus*. *Metoposaurus* appears to have been an aquatic animal that was little specialised
45 concerning feeding behaviour. This taxon may have used two foraging techniques in hunting; an
46 ambush strategy, using bilateral biting, or active hunting, using lateral strikes of the head.

47 However, microscopic data suggest that lateral biting was ~~commoner~~ than can be observed in
48 Finite Element Analysis only. The main factor that determined its mode of life probably was
49 water levels. During optimum water conditions, metoposaurids were active ambush predators
50 capable of lateral strikes of the head. The dry season required a less active mode of life with
51 particularly efficient bilateral biting and, combined with their characteristically anteriorly
52 positioned orbits, optimal for ambush strategy. This ability for food acquisition, independent of
53 environmental conditions, could be the key to explain the very common occurrence of
54 metoposaurids during the Late Triassic.

55

56 KEY WORDS

57 bone histology, dermal bone, FEA, feeding strategy, *Metoposaurus*, skull, suture morphology,
58 Temnospondyli

59

60

61

62

63

64

65

66

67

68

69

70

71

72

73

INTRODUCTION

74

75 Reconstruction of the behaviour and function of ancient organisms is one of the most interesting

76 tasks in palaeobiology, but at the same time the most hypothetical as ~~the direct evidences~~ are

77 only very rarely preserved. There are three possible ways to inferring function and behavior from

78 fossils - empirical evidence, comparison with modern analogs, and biomechanical modeling.

79 ~~Evidences~~ about biology of extinct taxa might be collected based on the morphological,

80 anatomical or microscopic characters of fossils themselves, but also important sources of the

81 information about lifestyle are sediments, associated ~~fossils or any traces~~. In the ideal model the

82 function or behavior proposed based on the collected ~~evidences~~ should be testable ~~in modern~~

83 ~~world~~. However, sometimes implications are limited as in the case of e.g., Temnospondyli

84 (*Sanchez et al.*, 2010), the giant terrestrial sauropod dinosaurs (e.g., *Erickson*, 2005; *Sander et*

85 *al.*, 2011), or some marine reptiles (*Chen et al.*, 2014a, b; *Cheng et al.*, 2014; *Chun Li et al.*,

86 2011, 2013, 2016; *Klein et al.*, 2015a,b; *Houssaye, Sander & Klein*, 2016; *Klein et al.*, 2016)

87 because of lack of modern analogues. In this case ~~might be helpful~~ phylogenetic bracket ~~where~~

88 the presence of some characters and thus indirect the function could be deduced from the

89 phylogenetic relation (*Witmer*, 1995). However, it is possible only for groups with well-known

90 evolutionary history and rich fossil records. The last way to gather information about moving parts

91 and skeletons are various biomechanical models (*Benton*, 2010), which flourished during last

92 years thank ~~to develop~~ of computing technologies.

93 Nevertheless, the main limitation of all studies on the fossilized animal is an inability to
94 test the created model ‘in vivo’ and thus each modelling implies assumptions and simplifications
95 which should be taken into account in the interpretation of results. Because of the influence of
96 simplifications to model construction has not yet been fully examined and is therefore poorly
97 understood (i.e., *Ross et al.*, 2005; *Kupczik et al.*, 2007; *Wang et al.*, 2010, 2012; *Cox et al.*,
98 2011; *Wood et al.*, 2011; *Bright*, 2012; *Fitton et al.*, 2012) the validation and testing the
99 reliability of results using sensitivity (*Walmsley et al.*, 2013; *McCurry, Evans & McHenry*, 2015)
100 and validity analysis (*Bright & Rayfield*, 2011) is necessary. These procedures however remain
101 difficult to realise for most of extinct groups because the amount of preserved information in
102 fossilised state is limited. This is why it is extremely and highly recommended to merge and
103 compare each available type of information sources for a well-known taxon, but so far no
104 previous studies have done this.

105 In this sense, *Metoposaurus krasiejowensis* (*Sulej*, 2002) from the Upper Triassic of
106 southwest Poland provides an excellent case study, in view of the sheer number of excellently
107 preserved specimens recovered as well as the extensive data set for this taxon (*Sulej*, 2002, 2007;
108 *Konietzko-Meier & Sander*, 2013; *Konietzko-Meier & Klein*, 2013; *Gruntmeier, Konietzko-Meier*
109 *& Bodzioch*, 2016; *Fortuny, Marcé-Nogué & Konietzko-Meier*, 2017).

110 Metoposaurids belong to Temnospondyli, one of the most diverse groups of early
111 tetrapods, which flourished worldwide during the Carboniferous, Permian, and Triassic periods,
112 and survived the Triassic-Jurassic extinction as relics in eastern Asia and Australia until the
113 Early Cretaceous (*Holmes & Carroll*, 1977; *Milner*, 1990; *Warren, Rich & Vickers-Rich*, 1997;
114 *Schoch*, 2013). The most characteristic and widely known part of the temnospondyl skeleton is
115 the skull. It is a flat structure with only a few fenestrae on the skull roof (for nares, orbits and, in

116 some capitosaur, for closed otic notch); the palatal side has many more openings: large
117 subtemporal windows, interpterygoid vacuities and choanas. **Despite the fact that temnospondyls**
118 **have been studied for over 150 years (huge teeth with a labyrinthodont structure were described**
119 **by Jaeger 1824, 1828), the extremely large fossil records, numerous queries as to their biology**
120 **and mode of life remain.** One of the crucial issues concerns their mode of feeding.

121 Temnospondyls were carnivorous, but whether they mainly used suction feeding and/or direct
122 biting is still unclear (*Milner & Sequeira, 1998; Warren, 2000; Steyer et al., 2006; Witzmann,*
123 *2006; Damiani et al., 2009; Maganuco et al., 2009; Fortuny et al., 2011*). Suction feeding was
124 possibly present in almost all larval temnospondyls, and many adult temnospondyl taxa with
125 well-ossified hyobranchial skeletons, i.e. plagiosaurs (*Damiani et al., 2009; Fortuny et al., 2011;*
126 *Witzmann & Schoch, 2013*). Other clades of temnospondyls (e.g. edopoids, eryopids and
127 stereospondylomorpha, including Archegosauriformes and Stereospondyli) have been
128 hypothesized to be feeding analogous to ~~the~~ crocodiles (*Milner & Sequeira, 1998; Warren, 2000;*
129 *Steyer et al., 2006; Witzmann, 2006; Maganuco et al., 2009; Fortuny et al., 2011, 2012*). These
130 interpretations are mostly inferred from morphological characters of skull, dentition and i.e.
131 presence of hyobranchial skeletons. Up to date only few very promising attempts of computer
132 modeling (finite element analysis and geometric morphometrics) were done (*Stayton & Ruta,*
133 *2006; Fortuny et al., 2011, 2012, 2016, 2017*). Despite the interesting conclusions it is important
134 to remember that, the computing models require a lot of methodological assumptions (see next
135 chapter) and the influence of the simplifications on the final model can lead to inaccuracies or
136 misinterpretations. Thus in the present study ~~is~~ for the first time correlation of histological and
137 cranial suture morphology results with computational biomechanics (FEA) is done. Merging
138 these three sources of data will first test the **correctness** of the biological reconstructions

139 generated by FEA and second give the new insights into the feeding ecology of Temnospondyli
140 in greater detail.

141

142 **TESTING FEEDING**

143

144 **Methodological approach to Finite Element Analysis**

145 A method which could help to understand the ecomorphological patterns of feeding is 3D Finite
146 Element Analysis (FEA). FEA documents deformation and distribution of strains and stresses in
147 these skulls that are related to different ecomorphologies (*Fortuny et al.*, 2011, 2012, 2016,
148 2017; *Lautenschlager, Witzmann & Werneburg*, 2016). Over recent years, FEA has been used
149 intensively to study the biomechanical behaviour of a wide array of vertebrates, providing new
150 insights into exploration of function, morphological evolution, particular adaptation and
151 biological structure constraints (*Rayfield*, 2007). FEA enables to obtain stress distribution
152 patterns that can be interpreted in order to understand either biomechanical behaviour or
153 evolutionary adaptation (*Witzel et al.*, 2011). It also allows to analyse and interpret parameters
154 such as stress and strain patterns indifferently on a qualitative comparative framework using
155 models of different shapes and sizes. It is important to note, that in FE analyses the stresses,
156 which is a physical quantity that expresses the internal forces that neighbouring particles of a
157 continuous material exert on each other, is described. However in the literature very often
158 interchangeably occurs the term strain, which is the measure of the deformation of the material.
159 This is possible and correct because both parameters are proportionally related by Hooke's Law
160 when linear properties of materials are assumed (see *Timoshenko*, 1976).

161 FEA studies could be approached from two different perspectives: deductive or inductive.
162 The deductive approach assumes a close relationship between form and function. This type of
163 analysis allows to manipulate FEA models digitally in order to alter the loading conditions or
164 add/ remove biological geometries, i.e., bone or pieces of bone or fill  any structure (e.g.,
165 *Marcé-Nogué et al.*, 2015). Alternatively, the inductive approach aims to test the relationship
166 between form and function, being able to test the assumption that form and function are tightly
167 linked (*Strait et al.*, 2005). However, a common limitation of FEA is the paucity of
168 biomechanical scenarios tested for each FEA (see *Fortuny et al.*, 2015 for a discussion), because
169 the behaviour of these animals probably included scenarios additional to the ones performed
170 there. Moreover, for any biological modelling which implies assumptions to perform any
171 analysis, these assumptions should be as minimal as possible and taken into account in the
172 interpretation of results. Furthermore, it should be borne in mind that modelling fossil taxa
173 implies even more assumptions as a result of the lack of data in the fossil record (*Anderson et al.*,
174 2012). Despite the mentioned problems, FE analyses are non-invasive, and thus irreplaceable and
175 crucial for examinations of the function of fossilized animals.

176

177 **Bone histology as a tool to test function**

178 Another approach to ensure reliable results and problem solving is the use of bone histology. The
179 bony framework is a product of biological optimisation and the bone structure is created to meet
180 local mechanical conditions. Thus, bone microstructure can be used to estimate local stress. Bone
181 histology seems to be an effective tool to reconstruct the biomechanical loading on the
182 structures; however it is a highly limited method because of its invasive nature.

183 Biomechanical properties of bone and biological implications have been extensively
184 analysed histologically (i.e., *Martin*, 1991; *Currey*, 2003, 2006, 2012; *Currey*, *Pitchford* &
185 *Baxter*, 2007; *Zioupos*, *Hansen* & *Currey*, 2008; *Mishra*, 2009; and references therein). Bone
186 microstructure is related directly to loads and can be modified during the animal's life time
187 (short-term adaptation) and/or on the long term, as an evolutionary adaptation. The mechanical
188 properties of bone are a result of a compromise between the need for a certain stiffness (i.e., to
189 reduce stress and achieve more efficient kinematics) and the need for enough ductility to absorb
190 impacts (i.e., to reduce the risk of fracture and minimise skeletal weight), but at the same
191 biological safety factors need to be maintained (*Biewener*, 1993).

192 Bone properties can be studied at four different levels: nanoscale (mineralised collagen fibres
193 and extrafibrillar minerals), microscale (microscopically visible structure), mesoscale (in
194 particular the relationship between cancellous and cortical bone) and the whole-bone scale
195 (*Currey*, 2012). In addition, biomechanical properties of bone may be described by different
196 variable indicators, such as Young's modulus of elasticity E , bending strength, determined in
197 tension, tensile strength or impact energy absorption of slotted specimens (*Currey et al.*, 2007)
198 and these depend directly of various biological and ecological factors during an animal's life. In
199 view of the fact that vertebrates are able to adapt their bone structure to imposed loading, this is a
200 highly complex issue (i.e., *Martin*, 1991; *Currey*, 2003, 2006, 2012; *Currey et al.*, 2007; *Zioupos*
201 *et al.*, 2008; *Mishra*, 2009). With strong simplification, the strength of a structure is the product
202 of organisational and compositional features (*Currey*, 2012). With regard to the mesoscale level,
203 the most important organisational feature is porosity, because bone loses strength and stiffness
204 with increased porosity. This is explained by the fact that soft tissues have essentially no strength
205 or stiffness with respect to non-hydrostatic stresses (*Martin*, 1991). However, high cortical

206 thickness can in part compensate for low resistance of bone tissue (*Carrier & Leon, 1990;*
207 *Margerie et al., 2004*). Compact bone is associated with high strength in tension, but
208 accompanied by a lack of strength in compression, which is higher for trabecular bone (*Martin,*
209 *1991; Currey, 2003; Rhee et al., 2009; Achrai & Wagner, 2013*). Considering composition,
210 lamellar bone with a regular orientation of collagen fibres is stronger than woven bone. In
211 lamellar bone the longitudinal fibres are associated with strength in tensions, while transverse
212 fibres are associated with strength in compression (*Martin, 1991; Currey, 2003*).

213 A significant portion of the early amphibian skeleton ~~is consisted~~ of dermal bone (skull,
214 mandible, clavicle and interclavicle), either intramembranous or metaplastic in origin. Dermal
215 bone, as a specific combination of trabecular and cortical bone, forms a “sandwich-type” or
216 plywood structure which is well known in engineering for its optimum structural properties
217 (*Currey, 2006*). In large flat bones which are bent along their shortest dimension, the cancellous
218 bone forms the middle of a sandwich, with the compact shell bearing the major loads and the
219 cancellous bone keeping the walls of the shell apart, and dealing with any shearing loads that
220 may arise. Dermal bone texture provides, moreover, a substantial increase in strength and
221 stiffness that is accompanied by a relatively small increase in mass (*Witzmann, 2009; Rinehart &*
222 *Lucas, 2013*). Calculations have demonstrated that there is a property/mass advantage, albeit
223 modest, in having cancellous bone in the middle, rather than having a solid, though overall
224 thinner bone (*Currey, 2006, 2012*). A mechanical advantage of metaplastic bone is a firm
225 connection between bone and overlying soft tissue, since the collagen fibres of the attached soft
226 tissue are confluent with the collagen fibres within the metaplastic bone (*Haines & Mohuiddin,*
227 *1968*).

228

229 **Role of the cranial suture in skull biomechanics**

230 The next important factor which should be taken into account during biomechanical analysis of a
231 skull is the type of cranial sutures. Cranial sutures are deformable joints between adjacent bones,
232 bridged by collagen fibres, and provide an ontogenetic and biomechanical function (*Jasinowski &*
233 *Reddy, 2012*). Their main purpose is to absorb or disperse stresses and strains in compression
234 and tension which act inside the skull or directly on its surface during activities related with
235 feeding, i.e., biting, mastication, holding struggling prey in the jaw and suction. Moreover,
236 cranial sutures resist stress rise during birth (mainly in mammals), during expansion of skull and
237 soft tissues, and absorbing impact forces (e.g., such as head butting in goats). The sutural
238 morphology is also an important indicator for deduction of the type of feeding (*Markey, Main &*
239 *Marshall, 2006*). *Markey et al.* (2006) distinguished three types of suture: interdigitated,
240 overlapping (or scarf) and abutting (or butt-ended). Each of these is responsible for counteracting
241 specific stress. Interdigitated sutures occur mainly in areas that experience compressive forces,
242 abutting (or butt-ended) sutures are associated with tensile strain, and variable strains (tension or
243 compression) counteract overlapping sutures (*Jasinowski, Rayfield & Chinsamy, 2010*). Rafferty
244 and Herring (1999) distinguished complex interdigitated sutures (associated with compressive
245 strain) and shallowly interdigitated or butt-ended sutures (associated with tensile strain).
246 Mechanical properties of cranial sutures have frequently been studied *in vivo* in extant
247 vertebrates, even in phylogenetically widely diverging groups that are adapted to life in different
248 environments (i.e., *Rafferty & Herring, 1999; Markey & Marshall, 2007a,b*). *Markey and*
249 *Marshall (2007a)* investigated cranial suture mechanics in the extant, suction-feeding fish
250 *Polypterus* and compared their results with cranial suture morphology in fossil vertebrates such
251 as the Devonian osteolepiform *Eusthenopteron*, the Devonian tetrapod *Acanthostega* and the

252 Triassic temnospondyl *Phonerpeton*. *Polypterus* exhibits tension-resistant sutures in the anterior
253 part of the skull (interfrontal suture) and compression-resistant sutures along the posterior skull
254 region (interparietal suture). *Eusthenopteron* shows the same pattern – tension-resistant suture
255 between frontals and compression-resistant suture between parietals, which suggest suction
256 feeding for this group (Markey & Marshall, 2007b). On the other hand, the terrestrial, bite-feeder
257 *Phonerpeton*, and the fully aquatic *Acanthostega*, exhibit similar compression-resistant sutures
258 between frontals and parietals (Markey and Marshall, 2007b). This suggests that even the fully
259 aquatic *Acanthostega* was adapted to feeding by biting (Markey and Marshall, 2007b).

260

261 **Interpretation of feeding behaviour of metoposaurids up to date**

262 Metoposaurids were common temnospondyls that were confined to the Upper Triassic, with
263 records from several continents (Sulej, 2007). Despite their common occurrence and well-known
264 *Bauplan*, the mode of life of metoposaurids still remains controversial. Earlier they were either
265 considered to have been passive bottom-dwellers in lakes and rivers, lying in wait for prey using
266 the passive “death-trap” model (Ochev, 1966; Murry, 1989), mid-water feeders, comparable to
267 temnospondyl capitosaur (Howie, 1970; Chernin and Cruickshank, 1978; Hunt, 1993) or active
268 swimmers that used limbs (Sulej, 2007) or tail (Konietzko-Meier, Bodzioch & Sander, 2013) for
269 propulsion.

270

271 **A cranial computational biomechanics approach based on Finite Element Analysis -**

272 The results and a discussion of FE models of the skull of *Metoposaurus krasiejowensis* have
273 recently been published by Fortuny et al. (2017). However, for easier understanding the
274 discussion a brief summary of the main results is included below.

275 Under bilateral biting, the model has showed moderate to low-level stresses on most parts
276 of the skull, with just a few peak stress levels in the posterior part (Fig. 1A). Small spots of stress
277 were present on the dorsal portion of the supratemporal and posterior part of the squamosal, but
278 mainly in ventral portions of the jugals and supratemporal and the posterior ramus of the
279 pterygoid. Of particular interest is the absence of stress around the premaxilla, the posterior part
280 of the maxilla and lacrimal and the naso-frontal region. Stress slightly increased around the
281 orbits. On the palate, a few peak levels of stress were present nearing the choanas, with no levels
282 of stress on the premaxilla, nor on most of the cultriform process and the parasphenoid.

283 The general pattern during lateral loading revealed low or absent levels of stress on the
284 skull roof; on the quadratojugal stress was slight (Fig. 1B). It is particularly significant that the
285 antorbital region had extremely low levels of stress. However, on the palate, the general stress
286 levels increase: low or moderate levels were seen on the vomer and premaxilla, while the
287 cultriform process presented low levels in its anterior part, being moderate in its posterior part
288 and absent from the central part. As far as the posterior part of the skull is concerned, high stress
289 levels were present on the posterior branch of the pterygoid and quadratojugals, while the
290 anterior part of the pterygoid had low or very low stress levels under lateral loading, while its
291 central area (adjacent to the parasphenoid) revealed moderate levels of stress. The major part of
292 the parasphenoid had moderate and high levels of stress, increasing on the posterior part of the
293 parasphenoid and in the exoccipitals.

294 The simulation of the skull raising system showed that the stress values are very low
295 along nearly the entire skull (Fig. 1C). The stress values increase only significantly in the
296 interorbital region, the regions around the otic notches, the central part of the cultriform process

297 and posterior rami of the pterygoids (Fig. 1C). Lower, but still measurable, stress is indicated in
298 the anterior rami of the pterygoid, ectopterygoid and in the vomer (Fig. 1C).

299 A 3D Finite Element Analysis of the metoposaur skull has revealed thus that the bottom
300 dweller and active predator hypotheses may ~~in part be joined~~ (Fortuny et al., 2017).
301 Metoposaurids preferred rapid bilateral biting which would confirm the ambush strategy –
302 resting on the bottom in wait for passing prey. However, the relatively low stress level that is
303 seen along the skull under lateral strike indicates that lateral strike of the head was possible, even
304 if this was not preferred (Fortuny et al., 2017). The FEA results also demonstrated clearly that
305 unilateral biting was avoided because the skull would experience a comparatively high stress
306 level, probably due to the absence of a secondary palate (Fortuny et al., 2016, 2017).

307 However, ~~how it~~ was mentioned above the FEA analysis has a limitation concerning the
308 amount of tested scenario. The results confirm the presence of direct lateral and bilateral biting,
309 but not exclude other combinations, except of unilateral biting, simple because of lack of models.
310

311 **Microscopic studies** - Cranial suture morphology and its predicted function for
312 *Metoposaurus* have been studied histologically in preliminary fashion (Gruntmejer, 2012). Most
313 of the sutures were defined as complex interdigitated which served a compression-resistant
314 purpose. Moreover, a shallowly interdigitated suture (prefrontal-lacrimal) has been observed,
315 which resisted tensile strains and two samples of probably overlapping sutures (maxilla-nasal
316 and frontal-postfrontal), which counter variable strains forces, have also be noted (Gruntmejer,
317 2012). Based on these facts, a predominant feeding mode of direct biting was concluded for
318 *Metoposaurus*. However, because of the presence of overlapping sutures in the anterior part of
319 the skull, capture of prey by suction could not be ruled out (Gruntmejer, 2012).

320

321

MATERIAL AND METHODS

322

323 **Material**

324 Two skulls of *Metoposaurus krasiejowensis* were analysed. One of these (UOPB 01029; 400 mm
325 in length) was studied histologically, while the second (UOPB 00124; 290 mm in length) was CT
326 scanned for 3D-Finite Element Analysis. Both specimens were collected at Krasiejów (southern
327 Poland) from the Upper Triassic (Norian according to recent stratigraphical studies: *Racki and*
328 *Szulc*, 2015; *Szulc, Racki & Jewuła*, 2015; *Szulc et al.*, 2015), lower bone bearing horizon (*sensu*
329 *Dzik and Sulej*, 2007), and are housed in the collections of Opole University (UOPB).

330

331 **Methods**

332 **Thin-sections** - The histological study of skull bones of *Metoposaurus krasiejowensis*
333 Skull UOPB 01029 has indicated a relatively stable collagen fibre pattern with parallel-fibred
334 bone constructing the grooves and inner cortex and lamellar bone present in the troughs/grooves
335 of the skull (*Gruntmejer et al.*, 2016). In contrast, microstructural characters (thickness and
336 compactness) change very clearly (*Gruntmejer et al.*, 2016), and thus may be used as a proxy to
337 estimate the mechanical loading. However, the detailed studies were not performed to analyse
338 the relations between the thicknesses, compactness and estimated biomechanical loading. It may
339 be assumed then that these characters influence the results of estimation significantly. This is
340 why these two features, based on the same thin-sections collection (Fig. 2) as published by
341 *Gruntmejer et al.* (2016) are ~~widely~~ analysed here and only these two were taken into account in

342 biomechanical simulation. Additionally, the thin-sections from the various border regions were
343 prepared to test the morphology of sutures (Fig. 2).

344 UOPB 01029 was sectioned in 39 places, inclusive of 19 flat dermal bones (Fig. 2),
345 according to standard petrographic procedures (*Chinsamy & Raath, 1992*). Non-dermal bones
346 such as exoccipital and quadratojugal were not analysed, because of their endochondral origin
347 and different shape. Cross-sectional shape morphology of cranial sutures was conducted on 26
348 thin sections (Table 1; green and purple lines in Fig. 2). The bone microstructure was studied in
349 16 thin sections (Table 2; red and purple lines in Fig. 2). Subsequently, the thin sections were
350 studied under a LEICA DMLP light microscope in normal and polarised light. Additionally,
351 cranial sutures were qualitatively analysed in Scanning Electron Microscope (SEM) to assess
352 their morphology.

353 In the thin sections, the average thickness of the entire bone was estimated, expressed as
354 an arithmetical average from three measurements of the thickness of the entire bone. The average
355 thickness of the bone was measured three times over the distance between the ventral side of the
356 bone and the bottom of troughs/grooves, and three times as the distance to the top of ridges. The
357 mathematical average was calculated from these measurements.

358 To estimate bone porosity the thin sections were scanned by Epson Scanner and
359 transformed into black and white images (Fig. 3). The analysis of compactness was done by
360 Bone Profiler (*Girondot & Laurin, 2003*).

361 In the prefrontal, squamosal 2 and parasphenoid, on account of the strongly variable bone
362 thickness, the significantly thinner parts of these bones (labelled in Figures 3 and 4 and in the
363 text as *b*, as opposed to the thicker part named *a*), were calculated separately (Fig. 3I,M and O).

364

365 **Finite Elements Analysis** - Skull UOPB 00124 (290 mm in length) was CT scanned for
366 3D-Finite Element Analysis. A Structural Static Analysis to evaluate the biomechanical
367 behaviour during biting and skull raising was performed using the Finite Element Package
368 ANSYS 14.5 in a Dell Precision™ Workstation T7600 with 32 GB (4X8GB) and 1600 MHz.
369 The detailed methodology was published by *Fortuny et al.* (2017). In this study the generated
370 models (*Fortuny et al.*, 2017; for summary see also chapter III) were reformulated in order to get
371 information about sutures function.

372

373

RESULTS

374

Biomechanical loading approach from thin-section analysis

375

376

377 **Bone microstructure** - The average thickness of dermal bones varies from 2 to 10 mm
378 (Table 2, Figs 3 and 4). In the posterior part of skull bones are the thickest (postparietal and
379 tabular), up to 10 mm with a compactness varying between 80 and 82%. The microstructural
380 characters indicate a very high biomechanical loading on this part of the skull (Table 2; Fig. 4).
381 The postorbital and jugal represent a similar average thickness (close to 7 mm), but the
382 compactness varies from 83% to 88%, respectively. These bones show a lower loading,
383 compared to the posterior part of skull, but still have high stress level. Further decrease of the
384 strength is observed for the lacrimal, quadratojugal, frontal and pterygoid bones, in which the
385 thickness oscillates around 6 mm and the compactness varies from 73 to 80% (Table 2; Figs 3
386 and 4). The postfrontal, squamosal 1, posterior part of squamosal 2, parietal and
387 supratemporal(a) present thicknesses of around four mm, with the compactness changing from

388 88 to 95% (Table 2; Figs 3 and 4). The nasal, prefrontal and parasphenoid(a) with a relatively
389 limited thickness and compactness received low biomechanical loads (Table 2; Figs. 3 and 4).
390 The vomer is extremely porous, with a compactness of only about 55%, accompanied by limited
391 thickness and possibly free of stress (Table 2, Figs 3 and 4). Markedly thinner are also medial
392 parts of the supratemporal and parasphenoid (Fig. 3 I and O). In these bones the thinnest
393 fragments are about 2 mm thick, contrary to the remaining part with an average thickness of
394 about 4 mm (Table 2, Figs 3 and 4). In squamosal 2 the decrease in bone thickness is more
395 gradual (Fig. 3M). In ~~all~~ these three bones the compactness increases along with thickness
396 decreasing, reaching more than 90% in the thinnest region. Despite the high compactness these
397 portions of bones are very weak, in view of their extreme thinness (Table 2, Figs 3 and 4).

398

399 **Cranial biomechanical loading approach from bone microstructure** - The
400 microstructural bone characters suggest a high biomechanical resistance of the posterior part of
401 the skull; this is moderate in the preorbital and along the lateral edges, with a tendency to
402 decrease in the otic notches region and postorbital area (Fig. 4). A slight increase of
403 biomechanical loading is present only next to the posterior margin of the orbits (Fig. 4). The
404 anterior part of squamosal 2 and the deep trough/groove in the supratemporal are considerably
405 weaker than in the remaining part of these bones. However, in the supratemporal there is a
406 narrow valley that represents a lateral canal (Fig. 3I). The squamosal 2 shows a gradual decrease
407 in mechanical resistance in an anterior direction, indicating low loading on the lateroposterior
408 part of the skull. The postfrontal, squamosal 1, posterior part of squamosal 2, parietal and
409 supratemporal(a) are thinner, but significantly more compact than the lacrimal, quadratojugal
410 and frontal and thus represent only a slight decrease of final biomechanical strength.

411 The bones from the palatal side represent moderate or low stress levels. Extremely weak
412 are the vomer and the medial part of the parasphenoid (Fig. 4), whereas the anterior branch of the
413 pterygoid shows a greater biomechanical resistance.

414

415 **Cranial suture morphology** - All sutures studied here are recognised as interdigitated.
416 The presence of this suture type has been noted in the anterior and posterior parts of the skull,
417 both on the skull roof and on the palatal side (Figs 5 and 6). Distinct clumps of Sharpey's fibres
418 occur along the lateral edges of bones (Fig. 7).

419

420 **Biomechanical role of sutures obtained from the FE analysis** - Under a bilateral
421 loading, results obtained for *Metoposaurus* reveal that the posterior sutures of the supratemporal,
422 in conjunction with the tabular, parietal and postparietal, and to a lesser extent the squamosal,
423 plays an important role in the absorption, flexion and distribution of stress in the posterior part of
424 the skull, where stresses are greater. With regard to the palate, the lateral extension of the jugal to
425 the anterior branch of the pterygoid, as well as the quadratojugal suture, probably also played an
426 important role in stress dissipation. To a lesser extent, the pterygoid-parasphenoid and sutures
427 around the choana played a minor role.

428

429 **DISCUSSION**

430

431 **New insights into skull biomechanics – merging methods**

432

433 **Bone histology vs computational biomechanics – how does bone structure correlate**
434 **with Finite Element Analysis?** - Values of equivalent Von Mises stresses and their distribution
435 were recorded in order to compare their behaviour under the effect of loads and constraints in the
436 bilateral and lateral cases. The Von Mises criterion is the most accurate for predicting fracture
437 location when isotropic material properties are used in cortical bone (*Doblaré, García & Gomez,*
438 2004). As stated previously, the von Mises stress patterns of the models could be used
439 indifferently with strain patterns, allowing to compare qualitatively these results with the
440 compactness obtained from histological thin sections.

441 The histological framework confirms mostly the stress distribution pattern obtained
442 during FE analyses. The histological characters support that the nasal and prefrontal are
443 relatively weak bones; thus, the biomechanical loading in these regions was relatively low. In
444 both simulations (bilateral and lateral) the same tendency is observed, with a slight increase of
445 stress level in the prefrontal (Fig. 8A and B), which is also thinner (Fig. 4). In the frontal region,
446 under a bilateral case, the estimated stress level exceeds that in the prefrontal and nasal (Fig.
447 8A). Histologically, the frontal is a relatively massive bone in comparison to the nasal and
448 prefrontal. This indicates that loading on the frontal region was high. The postfrontal, squamosal
449 2(a), parietal and squamosal 1 are thinner than the frontal, but more compact and thus the loading
450 could be the same or only slightly lower as on the frontal (Figs 3A-B and 4). The same tendency
451 is observed in bilateral and lateral FEA cases (Fig. 8A-B). Squamosal 2 is of special interest as
452 the FE models suggest a change of stress value from the posterior to the anterior part of this
453 element, receiving high to low levels, respectively (Fig. 8). Interestingly, the histological results
454 also reveal this change in the thickness of the cortex as well as in the porosity across the bone
455 (Fig. 4). Squamosal 2(b) in both FEA cases (bilateral and lateral) show barely any stress

456 anteriorly (Fig. 8A-B); moreover, histologically, squamosal 2(b) is a very thin bone, indicating
457 that the mechanical loading of this part of skull was very low, only slightly increasing posteriorly
458 (Fig. 4). In its entirety, the supratemporal is adapted to moderate loading (Fig. 4), which is
459 visible also in bilateral and lateral FEA cases (Fig. 8). The histological framework of the
460 supratemporal suggests that the most sensitive part of this bone, which represents a drastically
461 reduced strength, is the lateral line canal (Fig. 4). The increase in bone compactness visible in the
462 canal might partially compensate a decrease of bone thickness in this place. The lamellar bone
463 visible at the bottom of the canal (*Gruntmejer et al.*, 2016) is associated with marked strength of
464 this region but accompanied by low resistance in compression (*Martin*, 1991; *Currey*, 2003;
465 *Rhee et al.*, 2009; *Achrai & Wagner*, 2013). The significant change of microstructural conditions,
466 and thus biomechanical properties, shows that the lateral line canals might be crucial structures
467 for the biomechanical function of the skull; especially for metoposaurids with extremely deep
468 system of lateral canals.

469 The microstructure of the lacrimal, jugal and quadratojugal suggest a significantly high
470 loading on the lateral margins of the skull. The same tendency is visible in the lateral FEA case
471 (Fig. 8B), where an increase of stress level is suggested. It seems to be clearly connected with the
472 presence of tooth rows on the ventral side of these bones. The histological results in this case
473 suggest a commoner occurrence of lateral biting than is concluded only from Finite Element
474 Analysis.

475 For the tabular and postparietal, the histological analysis reveals that these elements are
476 biomechanically adapted to receive high amounts of stress (Fig. 4). Moreover, these bones are
477 strongly metaplastic, which suggest a tight connection to muscles or ligaments (*Gruntmejer et*
478 *al.*, 2016). Under bilateral and lateral FEA loadings, the skull region receives a low or moderate

479 level of stress (Fig. 8A-B). However, it should be noted that other variables affect tabular and
480 parotic process, otic notch and mainly the cleidomastoideus muscles related to skull raising (Fig.
481 8C). All these variables possibly could affect the biomechanical properties of this element, and
482 explain the strength and biomechanic capabilities found in the histological analysis.

483 With regard to the palatal side, the Finite Element loading cases suggest low stress for the
484 pterygoid, and slightly higher for the parasphenoid, which is in agreement with the
485 microstructural results (Figs. 4 and 8). Additionally, the histological framework suggests that the
486 parasphenoid was loaded more next to the external edges than near the central axis, where the
487 bone is thinnest. *Marcé-Nogué et al.* (2015) pointed out that during skull raising relatively high
488 stress affected the cultriform process. The histological results obtained herein do not appear to
489 support the idea of any high loading on the palatal side of the skull. However, the section was
490 done only from the very posterior part of the parasphenoid; the cultriform process itself was not
491 sectioned. Taking into account the high microstructural variability of skull bones (*Gruntmejer et*
492 *al.*, 2016) it cannot be ruled out that the anterior part of this bone is highly metaplastic. This,
493 along with large width of the process, might significantly increase the biomechanical strength of
494 this bone. To confirm this hypothesis more sections are needed. Otherwise, the Finite Element
495 lateral case shows a stress increase in the vomer (Fig. 8C), but this stress pattern is not supported
496 by the histological framework. The vomer is the weakest bone of the entire skull (Fig. 4).

497 The exoccipital and quadratojugal have an endochondral origin and develop via a
498 cartilage precursor. Histologically, both bones resemble the structure of vertebrae with a highly
499 trabecular domain surrounded by a thin, more compact cortex (*Konietzko-Meier et al.*, 2013).
500 Between the trabeculae the remains of calcified cartilage are visible suggesting slow ossification
501 of the endochondral region (*Konietzko-Meier et al.*, 2013; *Gruntmejer et al.*, 2016). However, in

502 both bones very strong Sharpey's fibres are present (*Gruntmejer et al.*, 2016). Large
503 concentrations of long, well-mineralised Sharpey's fibres in the exoccipital appear to represent
504 the remains of strong muscular attachments and ligaments that connect the skull to the vertebral
505 column that may have played a role during skull rising.

506

507 **The role of sutures in skull biomechanics** - All microscopically analysed cranial sutures
508 in an adult skull of *Metoposaurus* were defined as interdigitated, which served a compression-
509 resistant purpose. *Gruntmejer* (2012) previously, albeit erroneously, interpreted the morphology
510 of some sutures to be overlapping and shallowly interdigitated. However, the present histological
511 analysis reveals that all sutures are interdigitated (Figs. 5-7). Sutural morphology, unlike the very
512 variable bone histology, does not change along the skull. The histological results of cranial
513 suture morphology in *Metoposaurus* are the same as in the case of *Acanthostega*, i.e., the
514 presence of compression-resistant sutures both in the anterior and posterior parts of the skull
515 (Fig. 6). The absence of tension-resistant sutures between the frontals (commonly occurring in
516 aquatic suction-feeders) and a predominance of interdigitated sutures along the skull of
517 *Metoposaurus*, demonstrates that it had a biting behaviour.

518 The histological data confirm the estimates made for sutures on the basis of FEA
519 analysis. As previously discussed, FE results also reveal that unilateral strikes of the head were
520 probably not performed by metoposaurids (*Fortuny et al.*, 2017). In this respect, a correlation of
521 stress patterns and sutures also enforces this idea. Under unilateral biting (*Fortuny et al.*, 2017),
522 the high stress patterns correlate with the tabular-squamosal-supratemporal suture and, to a lesser
523 extent, with the postparietal and parietal but under this loading main stresses are seen in the
524 central part of the cultriform process, where no sutures are present. Moreover, this structure is

525 one of the most fragile ones of the metoposaurid skull. Finally, high stress levels under unilateral
526 loading are present in the parasphenoid plate whereas the parasphenoid-exoccipital suture could
527 have played a role, although great stress around the endocranial region suggests that this loading
528 was usually avoided. Lastly, under a lateral strike of the head, the high amount of stress
529 correlated with the quadrate-jugal, quadrate-pterygoid and parasphenoid-exoccipital sutures. This
530 loading was possibly less usual than the bilateral but most probably more optimal than unilateral
531 loading, in consideration of the suture pattern.

532

533 **New interpretation of mode of life**

534 Merging three different approaches (Finite Element Analysis, bone histology and cranial suture
535 morphology) provides data from different perspectives on skull biomechanics that, when
536 correlated yield, a clear image of the feeding behaviour of *Metoposaurus*. *Metoposaurus* appears
537 to have been an aquatic animal that could adapt to various environmental conditions and was less
538 specialised in the mode of feeding than assumed previously (Ochev, 1966; Murry, 1989; Howie,
539 1970; Chernin & Cruickshank, 1978; Hunt, 1993; Sulej, 2007). As suggested by Fortuny *et al.*
540 (2017), on the basis of Finite Element Analyses, metoposaurs could have used two foraging
541 techniques in hunting; an ambush strategy using bilateral biting was commonest, but active
542 hunting using lateral strikes of the head was also possible. However, on the basis of FE loading
543 cases (Fortuny *et al.*, 2017), unilateral biting was most probably excluded. The morphology of
544 sutures clearly indicates that suction feeding did not occur in *Metoposaurus*.

545 The microstructural structure of cranial bones mostly support the bilateral Finite Element
546 loading case, with the exception of the system of lateral canals, which does not appear to be well
547 adapted for handling high stress levels (Figs. 3I and 4).

548 However, microscopic data that indicate significantly high loading on the lateral margins
549 of the skull, suggest a ~~commoner~~ occurrence of lateral biting than is concluded from the Finite
550 Element Analysis only (Fig. 8). The main biting forces are connected with long rows of teeth
551 along the skull margin. These rows act actively with the tooth row in the dentary, which is
552 supported by the presence of sharp cutting edges on the tooth margin in dentary teeth (*Konietzko-*
553 *Meier & Wawro, 2007*). Important also is the role of the vomer tusk. As histology reveals, the
554 vomer is a very weak bone; on the basis of FEA, there was stress increase in the vomer during
555 lateral biting (absent under bilateral biting). At first view, this is contradictory. However, it may
556 indicate that the vomer tusks only played an active role in bilateral biting, but not in lateral biting
557 because it could easily have snapped.

558 The main factor that determines the mode of life probably is water level. The two-season
559 climate during the Late Triassic, with high and low water levels in local lakes and periodic rivers
560 (*Bodzioch & Kowal-Linka, 2012*) requires ecological strategies in order to survive the
561 unfavourable part (i.e., dry season) of the year. Among amphibians, the common strategy to wait
562 out the dry or cold season is aestivation/hibernation. However, the growth pattern preserved in
563 long bones (revealed by histology) of *Metoposaurus* does not show distinct, seasonal Lines of
564 Arrested Growth (LAGs) at all, but only zones and unusually thick annuli, which point to a
565 reduced growth rate for a certain period (*Konietzko-Meier & Klein, 2013; Konietzko-Meier &*
566 *Sander, 2013*). The numerous lines present in annulus indicate that animals reduced their activity
567 for several shorter periods but did not aestivate for the entire unfavourable time (*Konietzko-*
568 *Meier & Klein, 2013; Konietzko-Meier & Sander, 2013*). Growth, even slow, requires a regular
569 access to energy. Because of seasonally variable high and low water levels, also the feeding
570 strategies had to be adequate to counter environmental conditions. During favourable water

571 conditions metoposaurids may have been ambush and active predators capable of lateral strikes
572 of the head. The dry season required a less active mode of life with particularly efficient bilateral
573 biting, together with their characteristically anteropositioned orbits, optimal in ambush strategy.

574 Interestingly, the same feeding strategies were suggested for the small metoposaurid
575 *Apachesaurus* from North America (Fortuny *et al.*, 2017). Overall it could be concluded that
576 metoposaurids were well equipped for survival under various conditions, yet not specialised as
577 far as feeding strategies are concerned. This ability to acquire food independently of
578 environmental conditions could be the key character to guarantee the very common occurrence
579 of metoposaurids during the Late Triassic. However, the question remains why, in spite of their
580 wide adaptive strategies, they disappeared, together with other temnospondyl groups, at the end
581 of Late Triassic. Milner (1993, 1994) documented the demise of capitosaurids, metoposaurids
582 and laticopids at the Norian-Rhaetian boundary as a part of the end-Triassic extinction event
583 (ETE), considered to rank amongst the ‘Big Five’ mass extinctions. Global changes in
584 environmental and ecological conditions then were too much, even for the widely adaptive
585 *Metoposaurus*.

586

587

CONCLUSIONS

588 1. The histological analysis of skull microstructure and sutures morphology mostly confirm
589 the models created by FEA with the exceptions of the vomer which is histological a low
590 loaded bone, but in on the basis of FEA, there is a stress increase in the vomer during
591 lateral biting (absent under bilateral biting). Also the significant change of
592 microstructural conditions, and thus biomechanical properties, shows that the lateral line
593 canals might be crucial structures for the biomechanical function of the skull; especially

594 for metoposaurids with extremely deep system of lateral canals and should be considered
595 in the FEA modelling.

596 2. *Metoposaurus* have been an aquatic animal that could adapt to various environmental
597 conditions and was low specialised in the mode of feeding. It has used two foraging
598 techniques in hunting; an ambush strategy using bilateral biting and active hunting using
599 lateral strikes of the head. The morphology of sutures clearly indicates that suction
600 feeding did not occur in *Metoposaurus*.

601 3. The main factor that determines the mode of life probably is water level. During
602 favourable water conditions metoposaurids may have been ambush and active predators
603 capable of lateral strikes of the head. The dry season required a less active mode of life
604 with particularly efficient bilateral biting, together with their characteristically
605 anteropositioned orbits, optimal in ambush strategy.

606

607 **ACKNOWLEDGEMENTS**

608

609 J.F. is supported by a postdoc grant, “Beatriu de Pinos” 2014–BP-A 00048, from the Generalitat
610 de Catalunya; he also acknowledges the CERCA programme (Generalitat de Catalunya). J. M.-
611 N. is supported by the Deutsche Forschungsgemeinschaft (DFG, German Research Foundation,
612 KA 1525/9-2). We thank Hospital Mutua de Terrassa (Catalonia, Spain) for CT scanning of the
613 specimen. Caio Souto Maior (UPC) is acknowledged for his help with the segmentation of the
614 *Metoposaurus* specimen. We are grateful to John Jagt (Natuurhistorisch Museum Maastricht,
615 Nederland) for improving the English. D.K.-M. thanks Martin Sander for fruitful discussion and
616 support. We acknowledge Wiley publisher for figure permission. The journal editor (...) and

617 reviewers (...) are acknowledged for their comments which improved an earlier typescript
618 significantly.

619

620

REFERENCES

621

622 Achrai B & Wagner HD. 2013. Micro-structure and mechanical properties of the turtle carapace
623 as a biological composite shield. *Acta Biomaterialia* **9**:5890–5902.

624 Anderson PSL, Bright JA, Gill PG & Rayfield EJ. 2012. Models in palaeontological functional
625 analysis. *Biology Letters* **8**:119–122.

626 Benton M J. 2010. Studying function and behavior in the fossil record. *PLoS Biology* **8**:
627 e1000321.

628 Biewener AA. 1993. Safety factors in bone strength. *Calcified Tissue International and*
629 *Musculoskeletal Research* **53**: 68–74.

630 Bodzioch A & Kowal-Linka M. 2012. Unraveling the origin of the Late Triassic multitaxic bone
631 accumulation at Krasiejów (S Poland) by diagenetic analysis. *Palaeogeography*
632 *Palaeoclimatology Palaecology* **346/347**: 25–36.

633 Bright J A & Rayfield EJ. 2011. Sensitivity and ex vivo validation of finite element models of
634 the domestic pig cranium. *Journal of Anatomy* **219**: 456–471.

635 Carrier D & Leon LR. 1990. Skeletal growth and function in the California gull (*Larus*
636 *californicus*). *Journal of Zoology* **222**: 375–389.

637 Carroll RL & Holmes R. 1980. The skull and jaw musculature as guides to the ancestry
638 salamanders. *Zoological Journal of the Linnean Society* **68**: 1–40.

- 639 Chen X-H, Motani R, Cheng L, Jiang D-Y & Rieppel O. 2014a. The Enigmatic Marine Reptile
640 *Nanchangosaurus* from the Lower Triassic of Hubei, China and the Phylogenetic
641 Affinities of Hupehsuchia. *PLoS ONE* **9**: e102361.
- 642 Chen X-H, Motani R, Cheng L, Jiang D-Y & Rieppel O. 2014b. A Carapace-Like Bony ‘Body
643 Tube’ in an Early Triassic Marine Reptile and the Onset of Marine Tetrapod Predation.
644 *PLoS ONE* **9**: e94396.
- 645 Cheng L, Chen X-H, Shang Q-H & Wu X-C. 2014. A new marine reptile from the Triassic of
646 China, with a highly specialized feeding adaptation. *Naturwissenschaften* **101**: 251–259.
- 647 Chernin S & Cruickshank ARI. 1978. The myth of the bottom-dwelling capitosaur amphibians.
648 *South African Journal of Science* **74**: 111–112.
- 649 Chinsamy A & Raath MA. 1992. Preparation of fossil bone for histological examination.
650 *Palaeontologia Africana* **29**: 39–44.
- 651 Cox PG, Fagan MJ, Rayfield EJ & Jeffery N. 2011. Finite element modelling of squirrel, guinea
652 pig and rat skulls: using geometric morphometrics to assess sensitivity. *Journal of*
653 *Anatomy* **219**: 696–709.
- 654 Chun L, Rieppel O, Long C, & Fraser NC. 2016. The earliest herbivorous marine reptile and its
655 remarkable jaw apparatus. *Science Advances* **2**: e1501659.
- 656 Currey JD. 2003. The many adaptations of bone. *Journal of Biomechanics* **36**: 1487–1495.
- 657 Currey JD. 2006. *Bones: Structure and Mechanics*. Princeton University Press, Princeton.
- 658 Currey JD. 2012. The structure and mechanics of bone. *Journal of Materials Science* **47**: 41–54.
- 659 Currey JD, Pitchford J W & Baxter PD. 2007. Variability of the mechanical properties of bone,
660 and its evolutionary consequences. *Journal of the Royal Society Interface* **4**: 127–135.

- 661 Damiani R, Schoch RR, Hellrung H, Werneburg R & Gastou S. 2009. The plagiosaurid
662 temnospondyl *Plagiosuchus pustuliferus* (Amphibia: Temnospondyli) from the Middle
663 Triassic of Germany: Anatomy and functional morphology of the skull. *Zoological*
664 *Journal of the Linnean Society* **155**: 348–373.
- 665 Doblaré M, García JM & Gomez MJ. 2004. Modelling bone tissue fracture and healing: A
666 review. *Engineering Fracture Mechanics* **71**: 1809–1840.
- 667 Dzik J & Sulej T. 2007. A review of the early Late Triassic Krasiejów biota from Silesia, Poland.
668 *Palaeontologia Polonica* **64**: 3–27.
- 669 Erickson GM. 2005. Assessing dinosaur growth patterns: A microscopic revolution. *Trends in*
670 *Ecology & Evolution* **20**: 677–684.
- 671 Fitton LC, Shi JF, Fagan MJ & O’Higgins P. 2012. Masticatory loadings and cranial deformation
672 in *Macaca fascicularis* a finite element analysis sensitivity study. *Journal of Anatomy*
673 **221**: 55–68.
- 674 Fortuny J, Marcé-Nogué J, de Esteban-Trivigno S, Gil L & Galobart Á. 2011. Temnospondyli
675 bite club: ecomorphological patterns of the most diverse group of early tetrapods. *Journal*
676 *of Evolutionary Biology* **24**: 2040–2054.
- 677 Fortuny J, Marcé-Nogué J, Gil L & Galobart Á. 2012. Skull mechanics and the evolutionary
678 patterns of the otic notch closure in Capitosaurians (Amphibia: Temnospondyli). *The*
679 *Anatomical Record* **295**: 1134–1146.
- 680 Fortuny J, Marcé-Nogué J, Heiss E, Sanchez M, Gil L & Galobart Á. 2015. 3D Bite modeling
681 and feeding mechanics of the largest living amphibian, the chinese giant
682 salamander *Andrias davidianus* (Amphibia:Urodela). *PlosOne* **10**: e0121885.

- 683 Fortuny J, Marcè-Noguè J & Konietzko-Meier D. 2017. Feeding biomechanics of Late Triassic
684 metoposaurids (Amphibia: Temnospondyli): a 3D finite element analysis approach.
685 *Journal of Anatomy* **230**: 752–765.
- 686 Fortuny J, Marcè-Noguè J, Steyer JS, De Esteban-Trivigno S, Mujal E & Gil L. 2016.
687 Comparative 3D analyses and palaeoecology of giant early amphibians (Temnospondyli:
688 Stereospondyli). *Scientific Reports* **6**: 30387.
- 689 Girondot M & Laurin M. 2003. Bone Profiler: a tool to quantify, model, and statistically
690 compare bone-section compactness profiles. *Journal of Vertebrate Paleontology* **23**: 458–
691 461.
- 692 Gruntmejer K. 2012. Morphology and function of cranial sutures of the Triassic amphibian
693 *Metoposaurus diagnosticus* (Temnospondyli) from southwest Poland. In: *Krasiejów –*
694 *palaeontological inspirations* (eds E. Jagt-Yazykova , J. Jagt J, A. Bodzioch and D.
695 Konietzko-Meier), pp. 34–54. ZPW Plik, Bytom.
- 696 Gruntmejer K, Konietzko-Meier D & Bodzioch A. 2016. Cranial bone histology of
697 *Metoposaurus krasiejowensis* (Amphibia, Temnospondyli) from the Late Triassic of
698 Poland. *PeerJ* **4**: e2685.
- 699 Haines RW & Mohiuddin A. 1968. Metaplastic bone. *Journal of Anatomy* **103**: 527–538.
- 700 Holmes RB & Carroll RL. 1977. A temnospondyl amphibian from the Mississippian of Scotland.
701 *Bulletin of the Museum of Comparative Zoology* **147**: 489–511.
- 702 Houssaye A, Sander PM & Klein N. 2016. Adaptive Patterns in Aquatic Amniote Bone
703 Microanatomy—More Complex than Previously Thought. *Integrative and Comparative*
704 *Biology* **56**: 1349–1369.

- 705 Howie AA. 1970. A new capitosaurid labyrinthodont from East Africa. *Palaeontology* **13**: 210–
706 253.
- 707 Hunt AP. 1993. Revision of the Metoposauridae (Amphibia, Temnospondyli) and description of
708 a new genus from western North America. In: *Aspects of Mesozoic Geology and*
709 *Paleontology of the Colorado Plateau* (ed M. Morales), pp. 67–97. *Museum of Northern*
710 *Arizona Bulletin* **59**.
- 711 Jasinowski SC, Rayfield EJ & Chinsamy A. 2010. Functional implications of dicynodont cranial
712 suture morphology. *Journal of Morphology* **271**: 705–728.
- 713 Jasinowski SC & Reddy BD. 2012. Mechanics of cranial sutures during simulated cyclic loading.
714 *Journal of Biomechanics* **45**: 2050–2054.
- 715 Jäger GF. 1824. *De Ichthyosauri sive Proteosauri, Fossils, Speciminibus, in Agro Bollensi in*
716 *Wurtembergia Repertis*. Cotta, Stuttgart.
- 717 Jäger GF. 1828. *Über die fossile Reptilien, welche in Württemberg aufgefunden worden sind*. J.B.
718 Metzler, Stuttgart.
- 719 Klein N, Houssaye A, Neenan JM & Scheyer TM. 2015a. Long bone histology and
720 microanatomy of Placodontia (Diapsida: Sauropterygia). *Contributions to Zoology* **84**:
721 59–84.
- 722 Klein N, Voeten DFAE, Lankamp J, Jankamp J, Bleeker R, Sichelschmidt OJ, Liebrand M,
723 Nieweg DC & Sander PM. 2015b. Postcranial material of *Nothosaurus marchicus* from
724 the Lower Muschelkalk (Anisian) of Winterswijk, The Netherlands, with remarks on
725 swimming styles and taphonomy. *Paläontologische Zeitschrift* **89**: 961–981.

- 726 Klein N, Sander PM, Krahl A, Scheyer TM & Houssaye A. 2016 Diverse aquatic adaptations in
727 *Nothosaurus* spp. (Sauropterygia)—inferences from humeral histology and
728 microanatomy. *PLoS ONE* **11**: e0158448.
- 729 Konietzko-Meier D, Bodzioch A & Sander PM. 2013. Histological characteristics of the
730 vertebral intercentra of *Metoposaurus diagnosticus* (Temnospondyli) from the Upper
731 Triassic of Krasiejów (Upper Silesia, Poland). *Earth and Environmental Science*
732 *Transactions of the Royal Society of Edinburgh* **103**: 1–14.
- 733 Konietzko-Meier D & Klein N. 2013. Unique growth pattern of *Metoposaurus diagnosticus*
734 *krasiejowensis* (Amphibia, Temnospondyli) from the Upper Triassic of Krasiejów,
735 Poland. *Palaeogeography Palaeoclimatology Palaeoecology* **370**: 145–157.
- 736 Konietzko-Meier D & Sander PM. 2013. Long bone histology of *Metoposaurus diagnosticus*
737 (Temnospondyli) from the Late Triassic of Krasiejów (Poland) and its paleobiological
738 implications. *Journal of Vertebrate Paleontology* **35**: 1–16.
- 739 Konietzko-Meier D & Wawro K. 2007. Mandibular dentition in the Late Triassic temnospondyl
740 amphibian *Metoposaurus*. *Acta Palaeontologica Polonica* **52**: 213–215.
- 741 Kupczik K, Dobson CA, Fagan MJ, Crompton RH, Oxnard CE & O'Higgins P. 2007. Assessing
742 mechanical function of the zygomatic region in macaques: validation and sensitivity
743 testing of finite element models. *Journal of Anatomy* **210**: 41–53.
- 744 Lautenschlager S, Witzmann F & Werneburg I. 2016. Palate anatomy and morphofunctional
745 aspects of interpterygoid vacuities in temnospondyl cranial evolution. *The Science of*
746 *Nature* **103**: 79.

- 747 Li C, Jiang D-Y, Cheng L, Wu X-C & Rieppel O. 2013. A new species of *Largocephalosaurus*
748 (Diapsida: Saurosphargidae), with implications for the morphological diversity and
749 phylogeny of the group. *Geological Magazine* **151**: 100–120.
- 750 Li C, Rieppel O, Wu X-C, Zhao L-J, & Wang L-T. 2011. A new Triassic marine reptile from
751 southwestern China. *Journal of Vertebrate Paleontology* **31**: 303–312.
- 752 Maganuco S, Steyer JS, Pasini G, Boulay M, Lorrain S & Bénéteau A. 2009. An exquisite
753 specimen of *Edingerella madagascarensis* (Temnospondyli) from the Lower Triassic of
754 NW Madagascar; cranial anatomy, phylogeny, and restorations. *Memorie della Società
755 italiana di scienze naturali Milano* **36**: 1–72.
- 756 Marcé-Nogué J, Fortuny J, De Esteban-Trivigno S, Sánchez M, Gil L & Galobart À. 2015. 3D
757 Computational mechanics elucidate the evolutionary implications of orbit position and
758 size diversity of early amphibians. *PlosOne* **10**: e0131320.
- 759 Margerie E, Robin JP, Verrier D, Cubo J, Groscolas R & Castanet J. 2004. Assessing a
760 relationship between bone microstructure and growth rate: a fluorescent labelling study in
761 the king penguin chick (*Aptenodytes patagonicus*). *Journal of Experimental Biology* **207**:
762 869–879.
- 763 Markey MJ, Main RP & Marshall CR. 2006. *In vivo* cranial suture function and suture
764 morphology in the extant fish *Polypterus*: implications for inferring skull function in
765 living and fossil fish. *Journal of Experimental Biology* **209**: 2085–2102.
- 766 Markey MJ & Marshall CR. 2007a. Linking form and function of the fibrous joints in the skull: a
767 new quantification scheme for cranial sutures using the extant fish *Polypterus endlicherii*.
768 *Journal of Morphology* **268**: 89–102.

- 769 Markey MJ & Marshall CR. 2007b. Terrestrial-style feeding in a very early aquatic tetrapod is
770 supported by evidence from experimental analysis of suture morphology. *Proceedings of*
771 *the National Academy of Sciences of the United States of America* **104**: 7134–7138.
- 772 Martin RB. 1991. Determinants of the mechanical properties of bones. *Journal of Biomechanics*
773 **24**: 79–88.
- 774 Maxwell WD & Benton MJ. 1990. Historical tests of the absolute completeness of the fossil
775 record of tetrapods. *Paleobiology* **16**: 322–335.
- 776 McCurry MR, Evans AR & McHenry CR. 2015. The sensitivity of biological finite element
777 models to the resolution of surface geometry: a case study of crocodylian crania. *PeerJ* **3**:
778 e988.
- 779 Milner AR. 1990. The radiations of temnospondyl amphibians. In: *Major Evolutionary*
780 *Radiations* (eds P. D. Taylor and G.P Larwood), pp. 321–34. Clarendon Press, Oxford.
- 781 Milner AR. 1993. Biogeography of Palaeozoic tetrapods. In: *Palaeozoic Vertebrate*
782 *Biostratigraphy and Biogeography* (eds J. A. Long), pp. 324–353. Belhaven Press,
783 London.
- 784 Milner AR. 1994. Late Triassic and Jurassic amphibians: fossil record and phylogeny. In: *The*
785 *Shadow of the Dinosaurs: Early Mesozoic Tetrapods* (eds N. C. Fraser and H. D. Sues),
786 pp. 5–22. Cambridge University Press, Cambridge.
- 787 Milner AR & Sequeira SEK. 1998. A cochleosaurid temnospondyl amphibian from the Middle
788 Pennsylvanian of Linton, Ohio, U.S.A. *Zoological Journal of the Linnean Society* **122**:
789 261–290.
- 790 Mishra S. 2009. Biomechanical aspects of bone microstructure in vertebrates: potential approach
791 to palaeontological investigations. *Journal of Biosciences* **34**: 799–809.

- 792 Murry PA. 1989. Geology and paleontology of the Dockum Formation (Upper Triassic), west
793 Texas and eastern New Mexico. In: *Dawn of the age of dinosaurs in the American*
794 *Southwest* (eds S. G. Lucas and A. P. Hunt), pp. 102–144. Museum of Natural History,
795 Albuquerque, New Mexico.
- 796 Ochev VG. 1966. *Systematics and Phylogeny of Capitosauroid Labyrinthodonts*. Saratov State
797 University Press, Saratov. [in Russian].
- 798 Racki G, Szulc J. 2015. The bone-bearing Upper Triassic of Upper Silesia, southern Poland:
799 integrated stratigraphy, facies and events – introductory remarks. *Annales Societatis*
800 *Geologorum Poloniae* **85**: 553–555.
- 801 Rafferty KL & Herring SW. 1999. Craniofacial sutures: morphology, growth, and *in vivo*
802 masticatory strains. *Journal of Morphology* **242**: 167–179.
- 803 Rayfield EJ. 2007. Finite Element Analysis and Understanding the Biomechanics and Evolution
804 of Living and Fossil Organisms. *Annual Review of Earth and Planetary Sciences* **35**:
805 541–576.
- 806 Rhee H, Horstemeyer MF, Hwang Y, Lim H, Kadiri HE & Trim W. 2009. A study on the
807 structure and mechanical behavior of the Terrapene Carolina carapace: a pathway to
808 design bioinspired synthetic composites. *Materials Science and Engineering, C* **29**:
809 2333–2339.
- 810 Rinehart LF & Lucas SG. 2013. The functional morphology of dermal bone ornamentation in
811 temnospondyl amphibian. In: *The Triassic System* (eds L. H. Tanner, J.A. Spielmann and
812 S.G. Lucas), pp., 524–532. *New Mexico Museum of Natural History and Science, Bulletin*
813 **61**.

- 814 Ross CF, Patel BA, Slice DE, Strait DS, Dechow PC, Richmond BG. & Spencer MA. 2005.
815 Modeling masticatory muscle force in finite element analysis: sensitivity analysis using
816 principal coordinates analysis. *The Anatomical Record Part A Discoveries in Molecular
817 Cellular and Evolutionary Biology* **283A**: 288–299.
- 818 Sanchez S, Germain D, Ricqlès A de, Abourachid A, Goussard F, Tafforeau P. 2010. Limb–bone
819 histology of temnospondyls: implications for understanding the diversification of
820 palaeoecologies and patterns of locomotion of Permo–Triassic tetrapods. *Journal of
821 Evolutionary Biology* **3**: 2076–90.
- 822 Sander PM, Christian A, Clauss M, Fechner R, Gee C, Griebeler E-M, Gunga H-C, Hummel J,
823 Mallison H, Perry S, Preuschoft H, Rauhut O, Remes K, Tütken T, Wings O & Witzel U.
824 2011. Biology of the sauropod dinosaurs: the evolution of gigantism. *Biological Reviews
825 of the Cambridge Philosophical Society* **86**: 117–155.
- 826 Schoch RR. 2013. The evolution of major temnospondyl clades: an inclusive phylogenetic
827 analysis. *Journal of Systematic Palaeontology* **11**: 673–705.
- 828 Stayton CT & Ruta M. 2006. Geometric morphometrics of the skull roof of stereospondyls
829 (Amphibia: Temnospondyli). *Palaeontology* **49**: 307–337.
- 830 Steyer JS, Damiani R, Sidor CA, O’Keefe, FR, Larsson HCE, Maga A & Oumarou I. 2006. The
831 vertebrate fauna of the Upper Permian of Niger. IV. *Nigerpeton ricqlési* (Temnospondyli:
832 Cochleosauridae), and the Edopoid colonization of Gondwana. *Journal of Vertebrate
833 Paleontology* **26**: 18–28.
- 834 Strait DS, Wang Q, Dechow PC, Ross CF, Richmond BG, Spencer MA & Patel BA. 2005.
835 Modeling elastic properties in finite-element analysis: How much precision is needed to
836 produce an accurate model? *The Anatomical Record* **283A**: 275–287.

- 837 Sulej T. 2002. Species discrimination of the Late Triassic temnospondyl amphibian
838 *Metoposaurus diagnosticus*. *Acta Palaeontologica Polonica* **47**: 535–546.
- 839 Sulej T. 2007. Osteology, variability, and evolution of *Metoposaurus*, a temnospondyl from the
840 Late Triassic of Poland. *Palaeontologia Polonica* **64**: 29–139.
- 841 Szulc J, Racki G & Jewuła K. 2015. Key aspects of the stratigraphy of the Upper Silesian middle
842 Keuper, southern Poland. *Annales Societatis Geologorum Poloniae* **85**: 557–586.
- 843 Szulc J, Racki G, Jewuła K & Środoń A. 2015. How many Upper Triassic bone-bearing levels
844 are there in Upper Silesia (Southern Poland)? A critical overview of stratigraphy and
845 facies. *Annales Societatis Geologorum Poloniae* **85**: 587–626.
- 846 Timoshenko S. 1976. *Strength of Materials*. Van Nostrand, New York.
- 847 Walmsley CW, McCurry MR, Clausen PD & McHenry CR. 2013. Beware the black box:
848 investigating the sensitivity of FEA simulations to modelling factors in comparative
849 biomechanics. *PeerJ* **1**: e204.
- 850 Wang Q, Smith AL, Strait DS, Wright BW, Richmond BG, Grosse IR, Byron CD & Zapata U.
851 2010. The global impact of sutures assessed in a finite element model of a macaque
852 cranium. *The Anatomical Record* **293**: 1477–1491.
- 853 Wang Q, Wood SA, Grosse IR, Ross CF, Zapata U, Byron CD, Wright BW & Strait DS. 2012.
854 The role of sutures in biomechanical dynamic simulation of a macaque cranial finite
855 element model: implications for the evolution of craniofacial form. *The Anatomical*
856 *Record* **295**: 278–288.
- 857 Warren AA. 2000. Secondarily aquatic temnospondyls of the Upper Permian and Mesozoic. In:
858 *Volume 4* (eds H. Heatwole and R. L. Carroll), pp. 1121–1149. Beatty & Sons, Chipping
859 Norton.

- 860 Warren A, Rich T & Vickers-Rich PV. 1997 The last labyrinthodonts? *Palaeontographica*
861 *Abteilung A* **247**: 1–24.
- 862 Witmer LM. 1995. The Extant Phylogenetic Bracket and the importance of reconstructing soft
863 tissues in fossils. In: *Functional Morphology in Vertebrate Paleontology* (ed J. J.
864 Thomason), pp. 19 – 33. Cambridge University Press, Cambridge.
- 865 Witzel U, Mannhardt J, Goessling R, Micheli de P & Preuschoft H. 2011. Finite Element
866 Analyses and virtual syntheses of biological structures and their application to Sauropod
867 skulls. In: *Biology of Sauropod Dinosaurs. Understanding the Life of Giants* (eds N.
868 Klein, K. Remes, C. T. Gee and P. M. Sander), pp.171–196. Indiana University Press,
869 Bloomington and Indianapolis.
- 870 Witzmann F. 2006. Cranial morphology and ontogeny of the Permo-Carboniferous
871 temnospondyl *Archegosaurus decheni* Goldfuss, 1847 from the Saar–Nahe Basin,
872 Germany. *Earth and Environmental Science Transactions of the Royal Society of*
873 *Edinburgh* **96**: 131–162.
- 874 Witzmann F. 2009. Comparative histology of sculptured dermal bones in basal tetrapods, and the
875 implications for the soft tissue dermis. *Palaeodiversity* **2**: 233–270.
- 876 Witzmann F. & Schoch RR. 2013. Reconstruction of cranial and hyobranchial muscles in the
877 Triassic temnospondyl Gerrothorax provides evidence for akinetic suction feeding.
878 *Journal of Morphology*, **274**: 525–542.
- 879 Wood SA, Strait DS, Dumont ER, Ross CF & Grosse IR. 2011. The effect of modeling
880 simplifications on craniofacial finite element models: the alveoli (tooth sockets) and
881 periodontal ligaments. *Journal of Biomechanics* **44**: 1831–1838.

882 Zioupos P, Hansen U & Currey JD. 2008. Microcracking damage and the fracture process in
883 relation to strain rate in human cortical bone tensile failure. *Journal of Biomechanics* **41**:
884 2932–2939.

885

886

887

888

889

890

891

892

893

894

895

896

897

898

899

900

901

902

903

904

905

906 **Figure captions**

907

908 **Figure 1** Von Mises stress results (in MPa) of bilateral (A), lateral biting (B) and of skull raising
909 system (C) in *Metoposaurus krasiejowensis* (UOPB 00124). Image Credit: Journal of
910 Anatomy/Wiley.

911

912 **Figure 2** Skull of *Metoposaurus krasiejowensis* from the Upper Triassic of southwest Poland
913 (UOPB 01029) used in the histological study (A and B) and schematic drawings (C and D) of the
914 same with sectioning planes marked, in dorsal (A and C) and palatal views (B and D). In (C) and
915 (D), red lines indicate thin sections used in microstructural analysis; purple lines refer to thin
916 sections used in both microstructural analysis and cranial suture study; green lines indicate thin
917 sections used in cranial suture analysis. Scale bar equals 10 cm. Abbreviations: ec,
918 ectopterygoid; ex, exoccipital; f, frontal; j, jugal; l, lacrimal; m, maxilla; n, nasal; p, parietal; pf,
919 postfrontal; pl, palatinum; po, postorbital; pp, postparietal; prf, prefrontal; ps, parasphenoid; pt,
920 pterygoid; qj, quadratojugal; sq1, squamosal 1; sq2, squamosal 2; st, supratemporal; t, tabular; v,
921 vomer.

922

923 **Figure 3** General microstructure of skull bones of *Metoposaurus krasiejowensis* (UOPB 01029)
924 from the Upper Triassic of southwest Poland. A, nasal; B, postorbital; C, jugal; D, lacrimal; E,
925 prefrontal; F, parietal; G, postparietal; H, postfrontal; I, supratemporal; J, frontal; K, squamosal
926 1; L, tabular; M, squamosal 2; N, quadratojugal; O, parasphenoid; P, pterygoid; Q, vomer. Scale
927 bar equals 10 mm.

928

929 **Figure 4** Estimated biomechanical loading as reconstructed on the basis of microstructural
930 characters (average bone thickness vs compactness), on sectioned regions of the skull of
931 *Metoposaurus krasiejowensis* (UOPB 01029) from the Upper Triassic of southwest Poland. Note
932 that the estimated values are relative and show merely if loading on any given region was higher
933 or lower (on the scale bar from red to blue, respectively). It is not possible to calculate the
934 objective amount of stress in this case. Black bars inside colour ellipses indicate the sectioning
935 places; the ellipses without bars are symmetric to section areas.

936

937 **Figure 5** Microphotography and drawings illustrating the morphology of selected cranial sutures
938 in the skull of *Metoposaurus krasiejowensis* (UOPB 01029) from supplementary thin sections
939 between the postorbital - jugal (A), parietal - supratemporal (B), squamosal - jugal (C) and
940 pterygoid - exoccipital (D). Scale bar equals 1 mm. Abbreviations: Ex, exoccipital; J, jugal; P,
941 parietal; Po, postorbital; Pt, pterygoid; Sq, squamosal; St, supratemporal.

942

943 **Figure 6** Inferred strain patterns in the skull of *Metoposaurus krasiejowensis* (UOPB 01029)
944 from the Upper Triassic of southwest Poland, based on suture morphology.

945

946 **Figure 7** Histological framework of maxilla-vomer cranial suture in the skull of *Metoposaurus*
947 *krasiejowensis* (UOPB 01029) from the Upper Triassic of southwest Poland; image in plane
948 polarised light. White arrows indicate Sharpey's fibres.

949

950 **Figure 8** Von Mises stress results (in MPa) of bilateral (A), lateral biting (B) and of skull raising
951 system (C) in *Metoposaurus krasiejowensis* (UOPB 124) using a gape angle of 10 ° merged with
952 the model of biomechanical loading created on the basis of microstructural characters; skulls in
953 the background show FEA results; the outcome of histological reconstructions is illustrated as
954 oval forms, of different colours. Note that similar colours were used in FEA analysis and
955 histological estimates in order to illustrate how the general stress distribution in FEA and
956 histological analyses correlate; however, same colours do not signify the same stress values. In
957 FEA, the colours refer to objective values, while in histological models estimated values are
958 relative and show merely if the loading on any given region is higher or lower within a single
959 skull (on the scale bare from red to blue, respectively). Black bars inside colour ellipses indicate
960 the sectioning places; the ellipses without bars are symmetric to section areas. Image Credit for
961 FEA figure: Journal of Anatomy/Wiley.
962

Table 1 (on next page)

The cranial sutures analyzed in the skull of *Metoposaurus krasiejowensis* from Late Triassic of Poland.

1
 2 Table 1. The cranial sutures analyzed in the skull of *Metoposaurus krasiejowensis* from Late
 3 Triassic of Poland.

4

cranial sutures¹	number of samples
maxilla-nasal	1
maxilla-lacrimonal	2
maxilla-palatine	1
maxilla-vomer	1
vomer-palatine	2
interfrontal	2
frontal-postfrontal	1
jugal-postorbital	3
prefrontal-lacrimonal	1
parietal-supratemporal	2
supratemporal-squamosal	1
squamosal-jugal	1
interpostparietal	2
jugal-ectopterygoid	1
pterygoid-ectopterygoid	2
pterygoid-parasphenoid	2
pterygoid-exoccipital	2

5
 6 ¹For the detailed localization of the sections see Fig. 1 – green and purple lines.

7

Table 2 (on next page)

The thickness and compactness of the dermal skull bones of *Metoposaurus krasiejowensis* from Late Triassic of Poland.

¹The average thickness of entire bone was estimated in thin sections, expressed as an arithmetical average from three measurements of the thickness of a bone taken on the bottom of valleys and the top of ridges; ²Compactness was estimated using the software Bone Profiler (Girondot and Laurin, 2003).

- 1 Table 2. The thickness and compactness of the dermal skull bones of *Metoposaurus*
 2 *krasiejowensis* from Late Triassic of Poland.

bone	average thickness (μm) ¹	compactness (%) ²
nasal	4758	77.4
prefrontal	4256	78.5
lacrimal	5940	79.2
frontal	5549	76.3
postfrontal	3960	94.5
jugal	6940	87.8
postorbital	6940	82.6
parietal	3840	92.2
supratemporal (a)	4800	92.5
supratemporal (b)	2050	98.6
squamosal1	3915	89.1
squamosal2 (a)	4000	94.0
squamosal2 (b)	1600	98.7
quadratojugal	5610	78.6
postparietal	8670	80.7
tabular	10000	82.5
vomer	2925	54.7
parasphenoid (a)	4050	77.7
parasphenoid (b)	2100	91.0
pterygoid	5460	73.1

3

- 4 ¹The average thickness of entire bone was estimated in thin sections, expressed as an arithmetical
 5 average from three measurements of the thickness of a bone taken on the bottom of valleys and
 6 the top of ridges; ²Compactness was estimated using the software Bone Profiler (Girondot and
 7 Laurin, 2003).

8

9

10

11

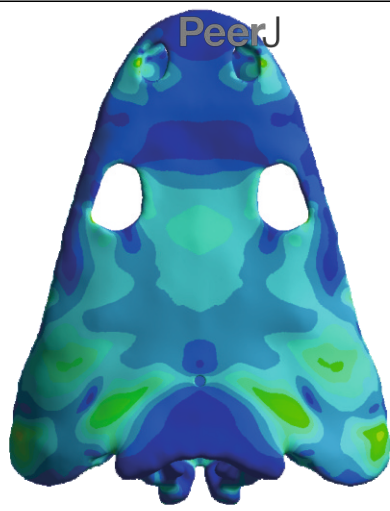
12

13

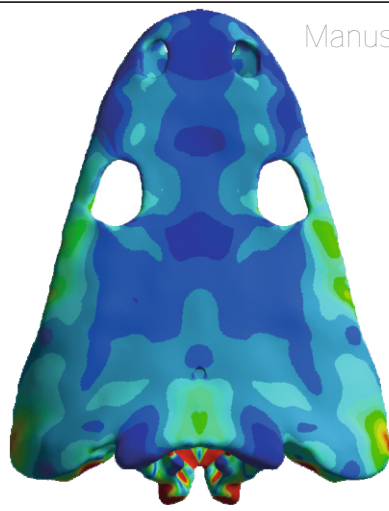
14

Figure 1(on next page)

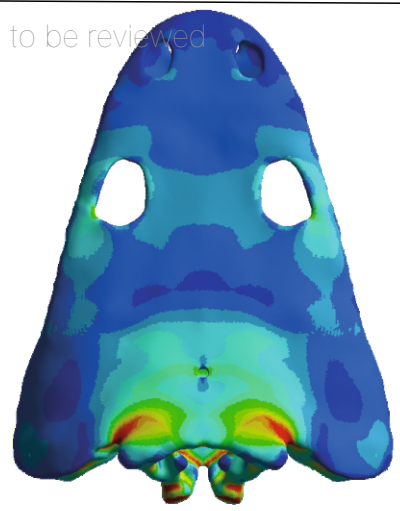
Von Mises stress results (in MPa) of bilateral (A), lateral biting (B) and of skull raising system (C) in *Metoposaurus krasiejowensis* (UOPB 00124). ImageCredit: Journal of Anatomy/Wiley.



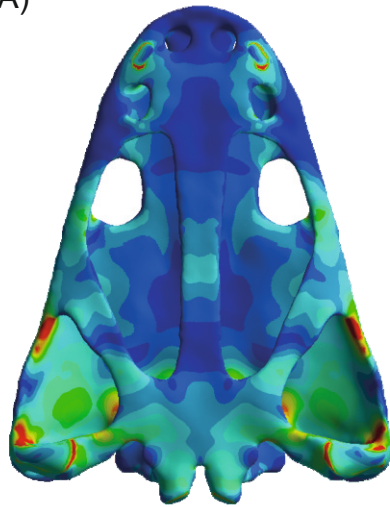
(A)



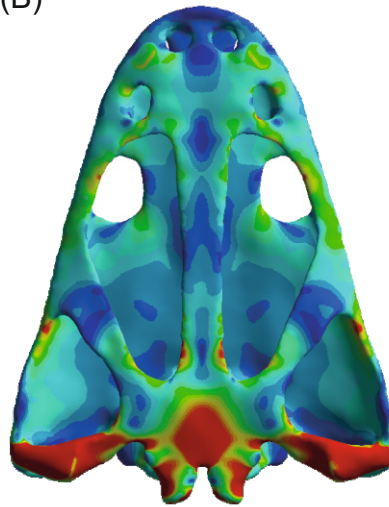
(B)



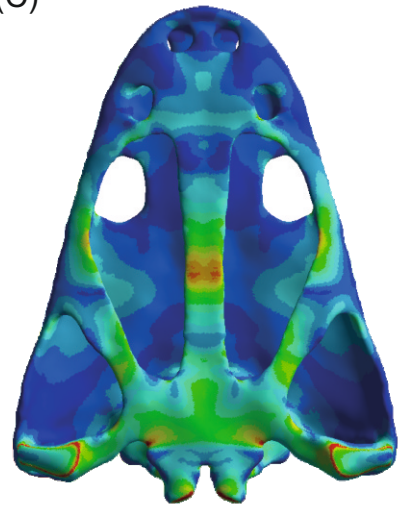
(C)



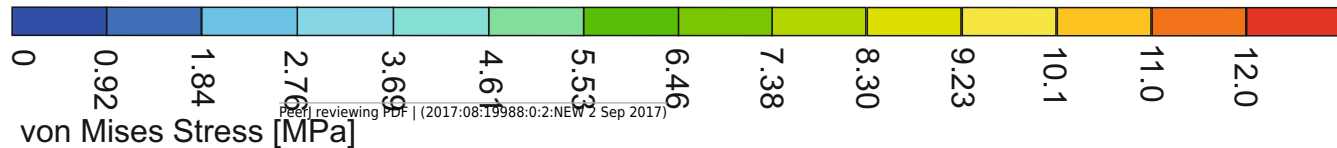
BILATERAL BITE



LATERAL BITE



SKULL-RAISING SYSTEM



von Mises Stress [MPa]

Figure 2(on next page)

Skull of *Metoposaurus krasiejowensis* from the Upper Triassic of southwest Poland (UOPB 01029) used in the histological study.

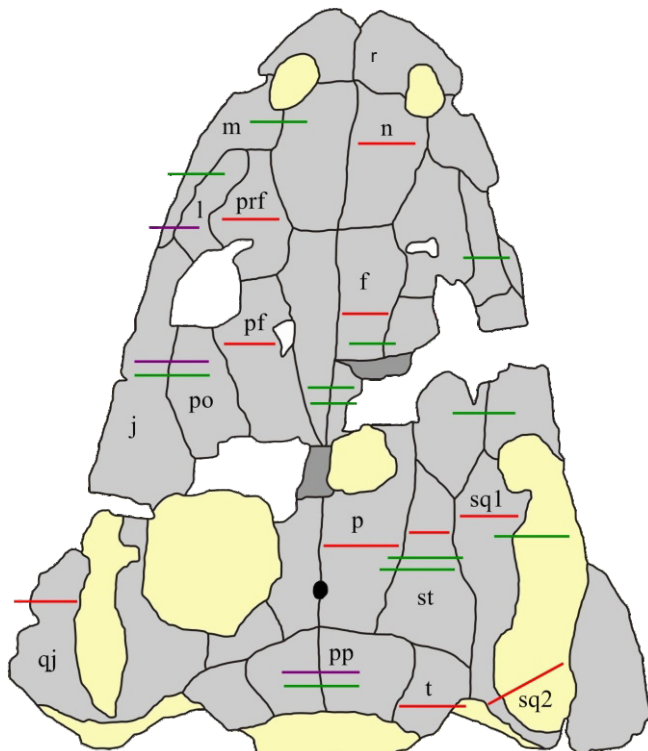
Skull of *Metoposaurus krasiejowensis* from the Upper Triassic of southwest Poland (UOPB 01029) used in the histological study (A and B) and schematic drawings (C and D) of the same with sectioning planes marked, in dorsal (A and C) and palatal views (B and D). In (C) and (D), red lines indicate thin sections used in microstructural analysis; purple lines refer to thin sections used in both microstructural analysis and cranial suture study; green lines indicate thin sections used in cranial suture analysis. Scale bar equals 10 cm. Abbreviations: ec, ectopterygoid; ex, exoccipital; f, frontal; j, jugal; l, lacrimal; m, maxilla; n, nasal; p, parietal; pf, postfrontal; pl, palatinum; po, postorbital; pp, postparietal; prf, prefrontal; ps, parasphenoid; pt, pterygoid; qj, quadratojugal; sq1, squamosal 1; sq2, squamosal 2; st, supratemporal; t, tabular; v, vomer



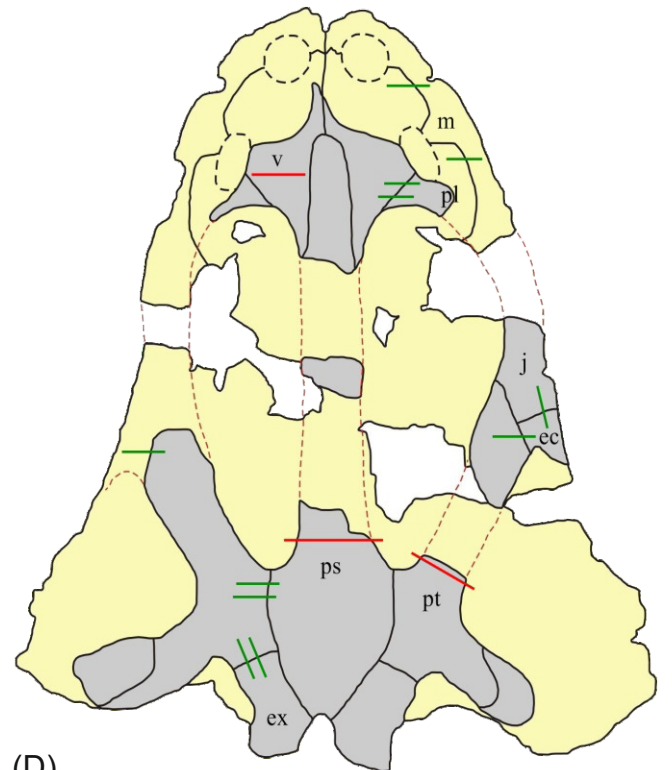
(A)



(B)



(C)



(D)

Figure 3(on next page)

General microstructure of skull bones of *Metoposaurus krasiejowensis* (UOPB 01029) from the Upper Triassic of southwest Poland.

A, nasal; B, postorbital; C, jugal; D, lacrimal; E, prefrontal; F, parietal; G, postparietal; H, postfrontal; I, supratemporal; J, frontal; K, squamosal 1; L, tabular; M, squamosal 2; N, quadratojugal; O, parasphenoid; P, pterygoid; Q, vomer. Scale bar equals 10 mm.

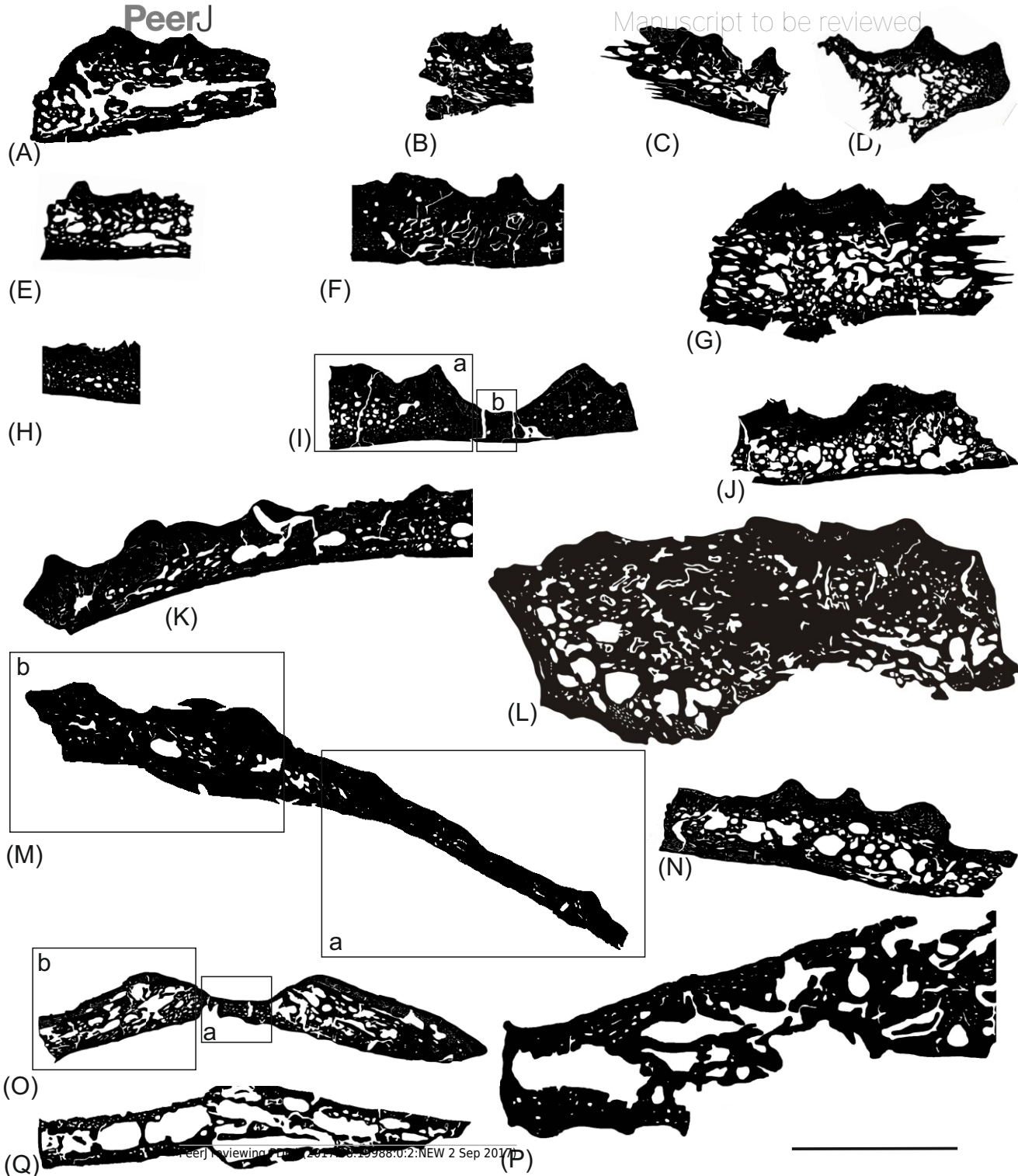
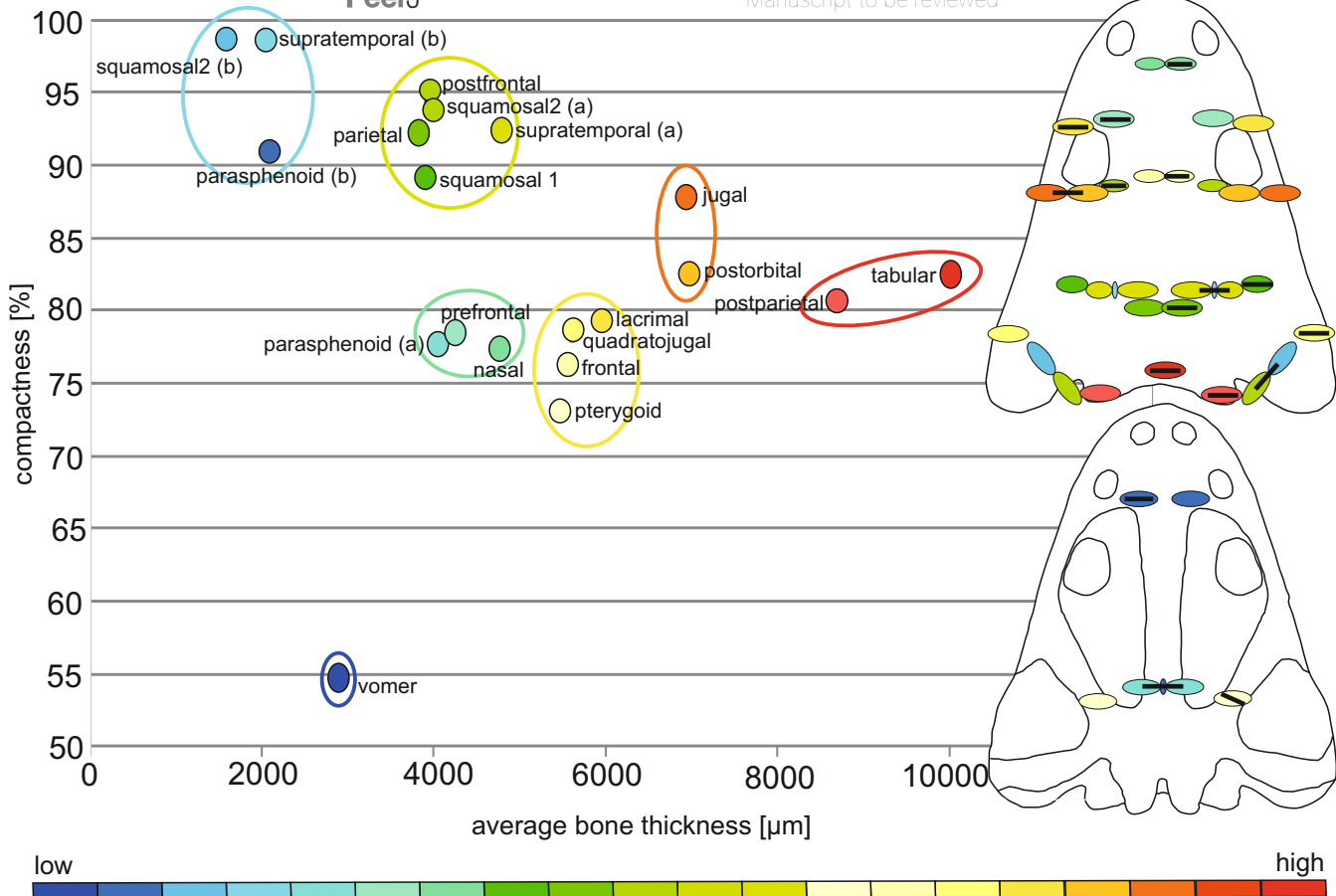


Figure 4(on next page)

Estimated biomechanical loading as reconstructed on the basis of microstructural characters (average bone thickness vs compactness), on sectioned regions of the skull of *Metoposaurus krasiejowensis*.

Estimated biomechanical loading as reconstructed on the basis of microstructural characters (average bone thickness vs compactness), on sectioned regions of the skull of *Metoposaurus krasiejowensis* (UOPB 01029) from the Upper Triassic of southwest Poland. Note that the estimated values are relative and show merely if loading on any given region was higher or lower (on the scale bar from red to blue, respectively). It is not possible to calculate the objective amount of stress in this case. Black bars inside colour ellipses indicate the sectioning places; the ellipses without bars are symmetric to section areas.



low

high

Figure 5(on next page)

Microphotography and drawings illustrating the morphology of selected cranial sutures in the skull of *Metoposaurus krasiejowensis*.

Microphotography and drawings illustrating the morphology of selected cranial sutures in the skull of *Metoposaurus krasiejowensis* (UOPB 01029) from supplementary thin sections between the postorbital - jugal (A), parietal - supratemporal (B), squamosal - jugal (C) and pterygoid - exoccipital (D). Scale bar equals 1 mm. Abbreviations: Ex, exoccipital; J, jugal; P, parietal; Po, postorbital; Pt, pterygoid; Sq, squamosal; St, supratemporal.

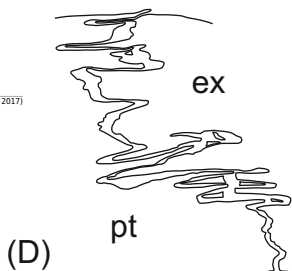
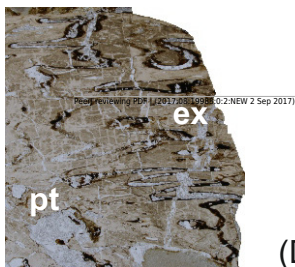
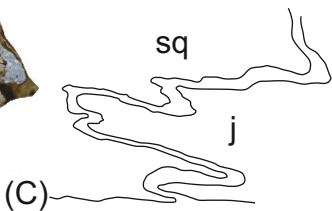
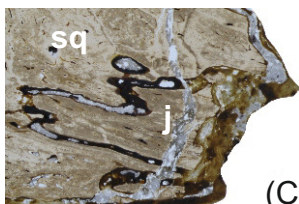
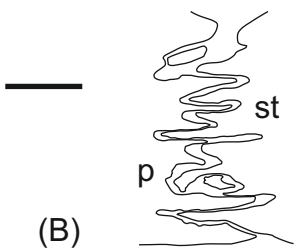
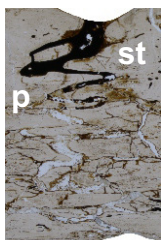
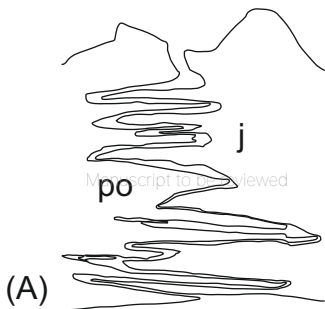
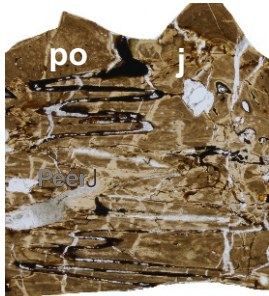
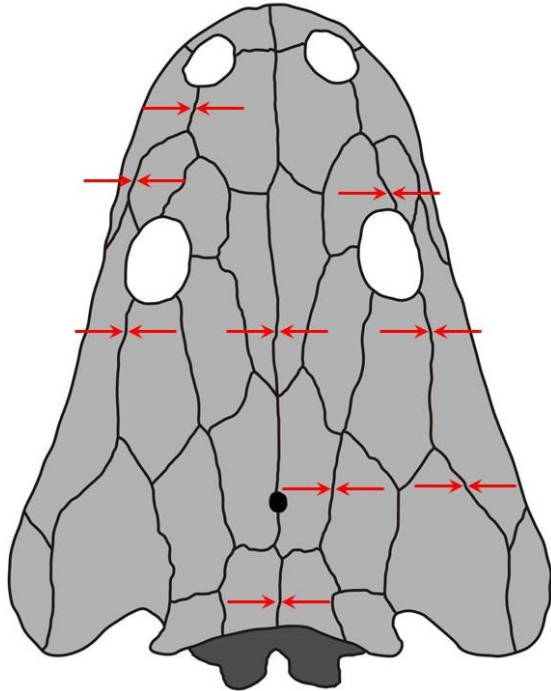


Figure 6 (on next page)

Inferred strain patterns in the skull of *Metoposaurus krasiejowensis* (UOPB 01029) from the Upper Triassic of southwest Poland, based on suture morphology.

(A)



(B)

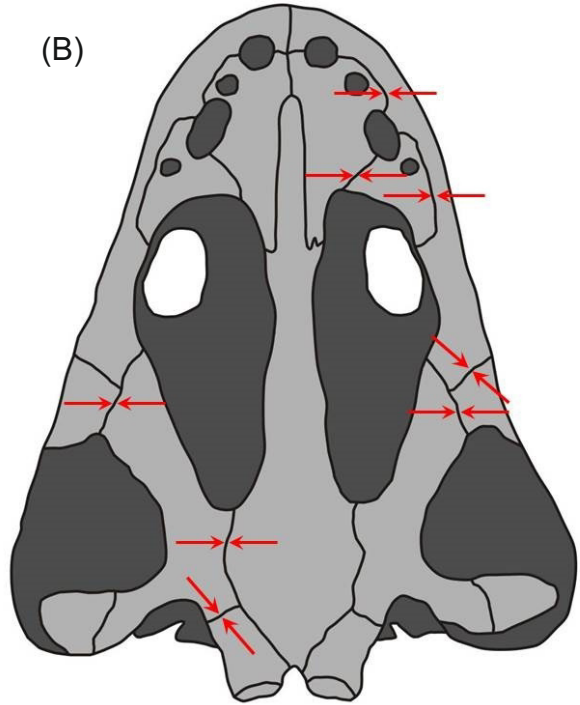


Figure 7 (on next page)

Histological framework of maxilla-vomer cranial suture in the skull of *Metoposaurus krasiejowensis* (UOPB 01029) from the Upper Triassic of southwest Poland, image in plane polarised light.

White arrows indicate Sharpey's fibres.

200 μm

PeerJ

Manuscript to be reviewed

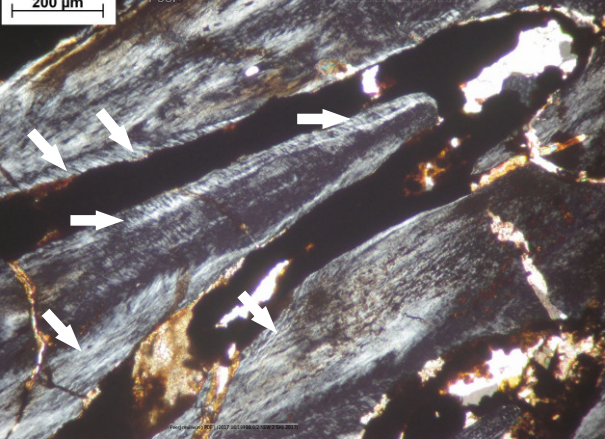
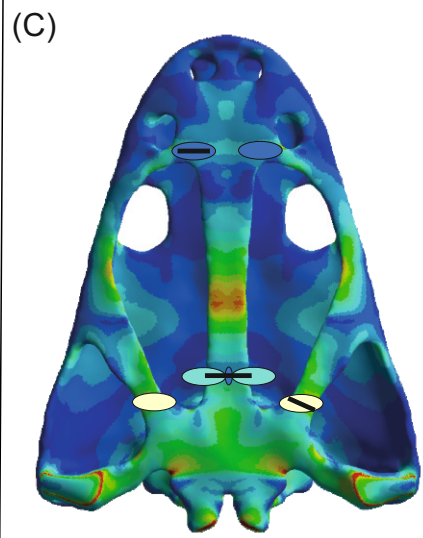
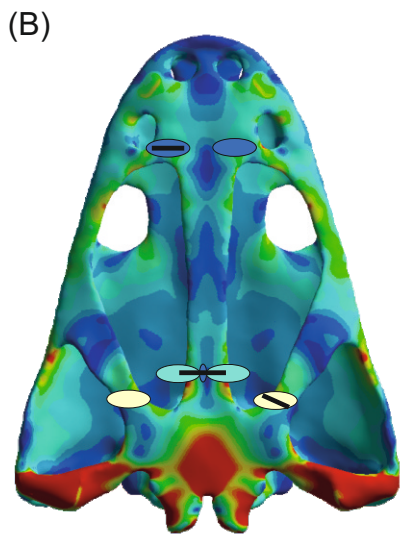
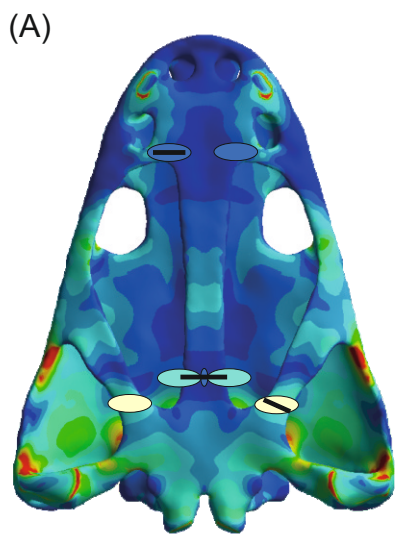
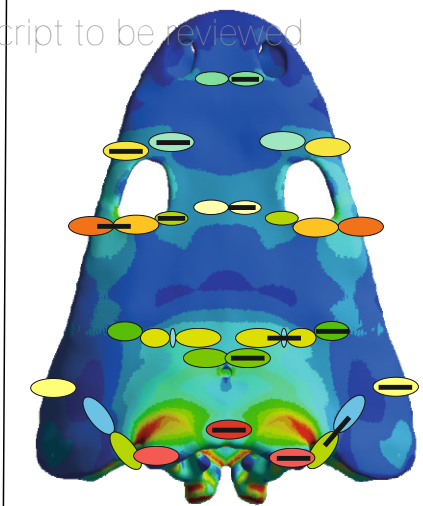
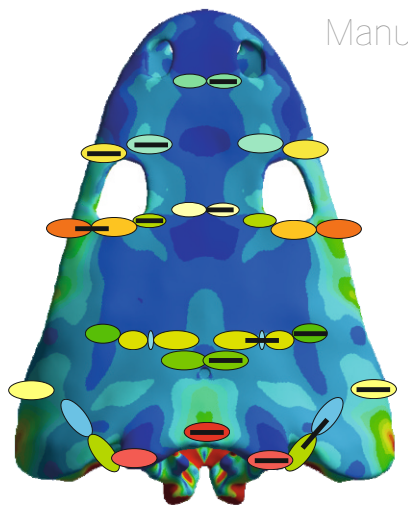
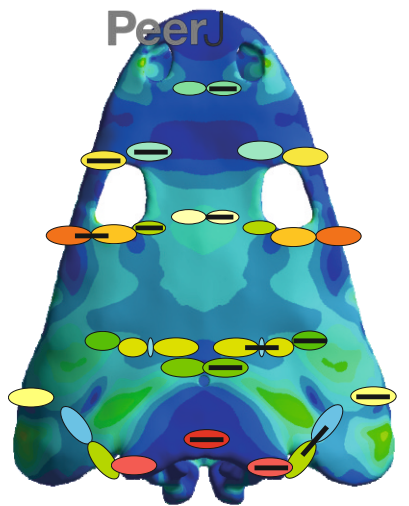


Figure 8(on next page)

Merging FEA with histology.

Von Mises stress results (in MPa) of bilateral (A), lateral biting (B) and of skull raising system (C) in *Metoposaurus krasiejowensis* (UOPB 124) using a gape angle of 10 ° merged with the model of biomechanical loading created on the basis of microstructural characters; skulls in the background show FEA results; the outcome of histological reconstructions is illustrated as oval forms, of different colours. Note that similar colours were used in FEA analysis and histological estimates in order to illustrate how the general stress distribution in FEA and histological analyses correlate; however, same colours do not signify the same stress values. In FEA, the colours refer to objective values, while in histological models estimated values are relative and show merely if the loading on any given region is higher or lower within a single skull (on the scale bare from red to blue, respectively). Black bars inside colour ellipses indicate the sectioning places; the ellipses without bars are symmetric to section areas.



BILATERAL BITE

LATERAL BITE

SKULL-RAISING SYSTEM



stress level as reconstructed from bone microanatomy

